Ticks and Tick-borne Diseases 14 (2023) 102161

Contents lists available at ScienceDirect

Ticks and Tick-borne Diseases

journal homepage: www.elsevier.com/locate/ttbdis

Original article

Mechanistic movement models to predict geographic range expansions of ticks and tick-borne pathogens: Case studies with *Ixodes scapularis* and *Amblyomma americanum* in eastern North America

Olivia Tardy [a,c,*], Emily Sohanna Acheson [a,c], Catherine Bouchard [a,c], Éric Chamberland [b], André Fortin [b], Nicholas H. Ogden [a,c], Patrick A. Leighton [a]

[a] Research Group on Epidemiology of Zoonoses and Public Health, Faculty of Veterinary Medicine, Université de Montréal, 3200 rue Sicotte, Saint-Hyacinthe, Quebec J2S 2M2, Canada
[b] Groupe Interdisciplinaire de Recherche en Éléments Finis (GIREF), Department of Mathematics and Statistics, Faculty of Science and Engineering, Université Laval, 1045 avenue de la Médecine, Quebec, Quebec, G1V 0A6, Canada
[c] Public Health Risk Sciences Division, National Microbiology Laboratory, Public Health Agency of Canada, 3200 rue Sicotte, Saint-Hyacinthe, Quebec, J2S 2M2, Canada

ARTICLE INFO

Keywords:
Amblyomma americanum
Borrelia burgdorferi sensu stricto
Climate warming
Ixodes scapularis
Reaction-advection-diffusion model
Spatial expansion

ABSTRACT

The geographic range of the blacklegged tick, *Ixodes scapularis*, is expanding northward from the United States into southern Canada, and studies suggest that the lone star tick, *Amblyomma americanum,* will follow suit. These tick species are vectors for many zoonotic pathogens, and their northward range expansion presents a serious threat to public health. Climate change (particularly increasing temperature) has been identified as an important driver permitting northward range expansion of blacklegged ticks, but the impacts of host movement, which is essential to tick dispersal into new climatically suitable regions, have received limited investigation. Here, a mechanistic movement model was applied to landscapes of eastern North America to explore 1) relationships between multiple ecological drivers and the speed of the northward invasion of blacklegged ticks infected with the causative agent of Lyme disease, *Borrelia burgdorferi* sensu stricto, and 2) its capacity to simulate the northward range expansion of infected blacklegged ticks and uninfected lone star ticks under theoretical scenarios of increasing temperature. Our results suggest that the attraction of migratory birds (long-distance tick dispersal hosts) to resource-rich areas during their spring migration and the mate-finding Allee effect in tick population dynamics are key drivers for the spread of infected blacklegged ticks. The modeled increases in temperature extended the climatically suitable areas of Canada for infected blacklegged ticks and uninfected lone star ticks towards higher latitudes by up to 31% and 1%, respectively, and with an average predicted speed of the range expansion reaching 61 km/year and 23 km/year, respectively. Differences in the projected spatial distribution patterns of these tick species were due to differences in climate envelopes of tick populations, as well as the availability and attractiveness of suitable habitats for migratory birds. Our results indicate that the northward invasion process of lone star ticks is primarily driven by local dispersal of resident terrestrial hosts, whereas that of blacklegged ticks is governed by long-distance migratory bird dispersal. The results also suggest that mechanistic movement models provide a powerful approach for predicting tick-borne disease risk patterns under complex scenarios of climate, socioeconomic and land use/land cover changes.

1. Introduction

Ticks are important vectors of many zoonotic pathogens that pose serious disease risks for human and domesticated animal populations (De La Fuente et al., 2008; Jongejan and Uilenberg, 2004). The number of human cases of tick-borne diseases is increasing worldwide (Madison-Antenucci et al., 2020), and this situation is exacerbated by geographic range expansion of ticks and the pathogens they transmit, particularly in northern latitudes (Sonenshine, 2018). The blacklegged tick (*Ixodes scapularis*), which was distributed through the eastern and the upper Midwest United States until early this century (Eisen et al., 2016), has expanded its range into southern parts of central and eastern

* Corresponding author.
E-mail address: olivia.tardy@umontreal.ca (O. Tardy).

https://doi.org/10.1016/j.ttbdis.2023.102161
Received 10 September 2022; Received in revised form 2 March 2023; Accepted 3 March 2023
Available online 28 March 2023

Canada (Ogden et al., 2014a). The lone star tick (*Amblyomma americanum*), which is established in the southeastern United States (Springer et al., 2014), has more recently been reported to be expanding its range into northern states (Fowler et al., 2022; Stafford et al., 2018) and southern Canada where adventitious ticks have been detected in passive tick surveillance (Nelder et al., 2019). The blacklegged tick is a vector of several human disease-causing pathogens, such as *Borrelia burgdorferi* sensu stricto (a spirochetal bacterium causing Lyme disease), *Anaplasma phagocytophilum* (the bacterium responsible for human granulocytic anaplasmosis), *Babesia microti* (the causative protozoan parasite of human babesiosis), *Ehrlichia muris eauclairensis* (a bacterium causing ehrlichiosis), *Borrelia miyamotoi* (a spirochetal bacterium causing a form of relapsing fever), and Powassan virus (the causative agent of Powassan virus disease) (Eisen and Eisen, 2018). The lone star tick also transmits multiple human pathogens, including *Ehrlichia chaffeensis* (the bacterium causing human monocytic ehrlichiosis), *Francisella tularensis* (the causative bacterium of tularemia), *Rickettsia rickettsii* (the bacterium responsible for Rocky Mountain spotted fever), Heartland virus (the causative agent of Heartland virus disease), and Bourbon virus (the causative agent of Bourbon virus disease) (Goddard and Varela-Stokes, 2009). It is also thought that repeated bites of lone star ticks can induce an allergy to red meat (Commins et al., 2011).

Among potential ecological drivers of the northward expansion of ticks and their pathogens, much attention has been given to climate change, especially increasing temperature (as reviewed in Gilbert, 2021; Ogden et al., 2021). Several dynamic and predictive models of blacklegged tick populations suggest that, under climate warming scenarios, this tick species will expand its latitudinal range beyond its current known geographic distribution into colder regions of Canada (McPherson et al., 2017; Ogden et al., 2005; Wu et al., 2013). For example, McPherson et al. (2017) predicted that Lyme disease risk will increase in several parts of southern Canada with climate warming even if greenhouse gas emissions were reduced enough to keep global warming below 2 °C. Similarly, climate warming is expected to cause the northward range expansion of the lone star tick, affecting southern Canada (Sagurova et al., 2019). As ticks spend more than 90% of their lifetime off a host (Needham and Teel, 1991), their survival and life cycle are greatly dependent on abiotic (e.g., temperature, humidity, and soil composition) and biotic (e.g., vegetation features, forest types, and host availability) conditions at a given spatial location (Mathisson et al., 2021; Ogden et al., 2021; Tsao et al., 2021). With a warming climate, ticks can benefit from reduced daily per capita mortality, prolonged duration of their questing activity seasons, and shortened life cycles (reviewed in Ogden et al., 2021).

Dispersal of ticks to new areas relies on the movement of their hosts (Tsao et al., 2021). Migratory birds can disperse infected ticks over long distances during their northward migration each year (Ogden et al., 2015), seeding new populations of ticks in previously unoccupied areas of the northern hemisphere as these areas become more climatically suitable, which results in an invasion that is "pulled" by founder tick populations (reviewed in Ogden et al., 2013b). At more local scales, ticks may be dispersed by movement of tick reproduction hosts (e.g., deer) and tick-borne pathogen reservoir hosts (e.g., rodents) within host home ranges, and also possibly spread more widely due to climate-driven shifts in host geographic ranges as warmer winters and longer vegetative growing seasons promote increasing host densities in the landscape (Dawe and Boutin, 2016; Roy-Dufresne et al., 2013). Together, these host movements would promote a "pushed" invasion of ticks at the edge of their current geographic range (reviewed in Ogden et al., 2013b). Effects of climate-induced changes in host distribution and abundance are difficult to predict for host-generalist ticks such as the blacklegged tick and lone star tick, which can switch host species in the face of host community composition changes (Eisen et al., 2017). Northward range spread of tick populations is likely driven by complex interactions between biotic and abiotic factors. The relationships between these factors and the speed of tick and tick-borne pathogen invasion have been studied empirically in the last decade (Leighton et al., 2012; Ogden et al., 2013a; Watts et al., 2018), but the impacts of mechanisms governing host movement are still unclear. To bridge this gap, we built a population-level model of the "reaction-advection-diffusion" type that simulates northward invasion of ticks and tick-borne pathogens over large spatial scales through the incorporation of a mechanistic formulation of host movement and a mate-finding Allee effect into tick population dynamics (Tardy et al., 2021). In a recent theoretical study, this model identified movement of migratory birds as an important driver of the northward spread of *I. scapularis* ticks infected with *B. burgdorferi* sensu stricto (Tardy et al., 2021).

In this study, we applied our reaction-advection-diffusion model to landscapes of eastern North America, and we integrated the effects of increasing temperature on tick population survival. To gain insight into the sensitivity of infected tick spread patterns to temperature increases, we conducted simulation experiments with two objectives: 1) to quantify the relative importance of each model input parameter and to identify their relationships with the speed of invasion by infected ticks, tick infection prevalence, and density of infected ticks from a global sensitivity analysis, and 2) to explore the capacity of the model to simulate northward range expansion of ticks and tick-borne pathogens in eastern North America under theoretical scenarios of increasing temperature (i.e., increases of 100, 200, 400 and 600 degree-days to baseline annual cumulative degree-days above 0 °C). The model was parameterized for blacklegged ticks infected with *B. burgdorferi* sensu stricto (i.e., encompassing range expansion of both ticks and the bacterium), and for lone star ticks without inclusion of pathogens transmitted by this tick.

2. Materials and methods

In this section, we first provide an overview of the original reaction-advection-diffusion model (Section 2.1), followed by model updates (Section 2.2). We then describe model parameterization (Section 2.3), model inputs and outputs (Section 2.4), model initialization (Section 2.5), sensitivity analysis (Section 2.6), and model validation (Section 2.7). A detailed description of the model is provided in Tardy et al. (2021).

2.1. Model overview

The model is based on a system of partial differential equations (PDEs) to account for tick movement by migratory birds and terrestrial hosts across spatially heterogeneous landscapes during three activity periods of migratory birds (northward migration in spring, breeding in spring and summer, and southward migration in late summer and autumn) where ticks are active. The model simulates densities (/km^2) of four population classes at location $\mathrm{x} = (x, y)$ at time t: 1) a population of ticks (T) including both immature and adult tick life stages, 2) a population of pathogen amplification hosts (i.e., hosts that can efficiently infect ticks; A), 3) a population of pathogen dilution hosts (i.e., hosts that infect ticks at lower rates than amplification hosts or do not infect them; D), and 4) a population of tick reproduction hosts, upon which adult ticks feed (R). In nature, the next generation of larval ticks is produced from eggs laid by adult female ticks. To describe infection dynamics, the populations of ticks, amplification hosts and dilution hosts are divided into susceptible (i.e., uninfected; S) and infected (I) classes, so that the total density of ticks, amplification hosts or dilution

hosts is $N = S + I$. The population of tick reproduction hosts consists of a single class that represents the total density of reproduction hosts (N_R). The model does not explicitly incorporate tick life stages to reduce computational complexity (e.g., convergence of numerical solutions), but we considered important tick life-history characteristics such as 1) adult ticks feeding on tick reproduction hosts (e.g., deer) contribute to the production of new ticks, and 2) tick infection with *B. burgdorferi* sensu stricto occurs when immature ticks feed on pathogen amplification hosts (e.g., rodents) and pathogen dilution hosts (e.g., possibly some bird species; Dumas et al., 2022). The system of PDEs describing the processes of tick and host population dynamics, as well as infection dynamics, has the following form:

Ticks:

$$\frac{\partial S_T(\mathrm{x},t)}{\partial t} = \underbrace{b_{Allee}(N_T)N_T}_{\text{Birth}} - \underbrace{m_{Allee}(N_T)S_T}_{\text{Death}} - \underbrace{\lambda_T S_T}_{\text{Infection}} + \underbrace{\nabla\cdot(D_T\nabla S_T)}_{\substack{\text{Random (diffusive) movement}\\ \text{of ticks by hosts associated}\\ \text{with a resource gradient}}} - \underbrace{\nabla\cdot\left(\overrightarrow{C_T}S_T\right)}_{\substack{\text{Directed (advective) movement}\\ \text{of ticks by hosts associated}\\ \text{with a resource gradient}}},$$

$$\frac{\partial I_T(\mathrm{x},t)}{\partial t} = \underbrace{\lambda_T S_T}_{\text{Infection}} - \underbrace{m_{Allee}(N_T)I_T}_{\text{Death}} + \underbrace{\nabla\cdot(D_T\nabla I_T)}_{\substack{\text{Random (diffusive) movement}\\ \text{of ticks by hosts associated}\\ \text{with a resource gradient}}} - \underbrace{\nabla\cdot\left(\overrightarrow{C_T}I_T\right)}_{\substack{\text{Directed (advective) movement}\\ \text{of ticks by hosts associated}\\ \text{with a resource gradient}}},$$

Pathogen amplification hosts:

$$\frac{\partial S_A(\mathrm{x},t)}{\partial t} = \underbrace{b_A\left(1-\frac{r_A}{b_A K_A}S_A\right)N_A}_{\text{Birth}} - \underbrace{d_A S_A}_{\text{Death}} - \underbrace{\lambda_A S_A}_{\text{Infection}},$$

$$\frac{\partial I_A(\mathrm{x},t)}{\partial t} = \underbrace{\lambda_A S_A}_{\text{Infection}} - \underbrace{\left(d_A + \frac{r_A}{K_A}N_A\right)I_A}_{\text{Death}},$$

Pathogen dilution hosts:

$$\frac{\partial S_D(\mathrm{x},t)}{\partial t} = \underbrace{b_D\left(1-\frac{r_D}{b_D K_D}S_D\right)N_D}_{\text{Birth}} - \underbrace{d_D S_D}_{\text{Death}} - \underbrace{\lambda_D S_D}_{\text{Infection}},$$

$$\frac{\partial I_D(\mathrm{x},t)}{\partial t} = \underbrace{\lambda_D S_D}_{\text{Infection}} - \underbrace{\left(d_D + \frac{r_D}{K_D}N_D\right)I_D}_{\text{Death}},$$

Tick reproduction hosts:

$$\frac{\partial N_R(\mathrm{x},t)}{\partial t} = \underbrace{r_R\left(1-\frac{N_R}{K_R}\right)N_R}_{\text{Birth}}.$$

Here, $S_T(\mathrm{x},t)$, $I_T(\mathrm{x},t)$, $S_A(\mathrm{x},t)$, $I_A(\mathrm{x},t)$, $S_D(\mathrm{x},t)$, $I_D(\mathrm{x},t)$ and $N_R(\mathrm{x},t)$ represent the density of susceptible ticks, infected ticks, susceptible amplification hosts, infected amplification hosts, susceptible dilution hosts, infected dilution hosts and the total density of reproduction hosts, respectively, at spatial location $\mathrm{x} = (x, y)$ in the landscape at time t.

Tick population dynamics. In the model, the tick population is subject to a mate-finding Allee effect (i.e., difficulty for female and male ticks to find one another to mate at low population density). In the functions of density-dependent per capita birth $b_{Allee}(N_T)$ and mortality $m_{Allee}(N_T)$ of the model with the Allee effect, the parameter $a_T > 0$ adjusts the maximum per capita tick population growth rate, and the parameters $e_T \geq 0$ and $c_T \geq 0$ determine the effects of density-dependence and density-independence in the demographic functions, respectively (Hilker et al., 2007). The birth and mortality functions, and their associated parameters have the following form:

$$b_{Allee}(N_T) = a_T\left[-N_T^2 + (K_{T+} + K_{T-} + e_T)N_T + c_T\right],$$

$$m_{Allee}(N_T) = a_T(e_T N_T + K_{T+}K_{T-} + c_T),$$

$$\text{with } a_T = \frac{r_T}{K_{T+}^2},\ e_T = K_{T+},\ c_T = \frac{d_T}{a_T} - K_{T+}K_{T-},\ \text{and } r_T = \alpha_{TR}\left(\frac{N_R}{N_A+N_D+N_R}\right)B_T.$$

The parameter $K_{T+} > 0$ is the carrying capacity of ticks (/km^2), K_{T-} with $0 < K_{T-} < K_{T+}$ represents the minimum viable tick population density (/km^2) below which a pathogen-free tick population is expected to go extinct. In general, carrying capacity represents the maximum number of individuals of a species population that an environment can sustain for an indefinite period of time given resource availability (e.g., food, shelter, space) (Begon et al., 1996). The parameter d_T corresponds to the daily per capita mortality rate of ticks. The parameter r_T that characterizes the maximum per capita tick population growth rate without the Allee effect (/day) is defined as the product of the daily rate at which adult ticks (whose number of individuals is given by $n_a N_T$, where n_a is the proportion of adult ticks in the environment) encounter tick reproduction hosts R (α_{TR}), the proportion of tick reproduction hosts $\left(\frac{N_R}{N_A+N_D+N_R}\right)$, and the daily number of eggs produced per fed adult female tick (B_T). All ticks are born susceptible to infection. The calculation details for the parameters a_T, e_T and c_T can be found in Tardy et al. (2021).

Host population dynamics. In addition, each population of hosts of type H (i.e., $H = A$ for pathogen amplification hosts, $H = D$ for pathogen dilution hosts, and $H = R$ for tick reproduction hosts) follows a logistic growth with maximum per capita growth rate r_H and carrying capacity K_H. Carrying capacities of hosts vary according to habitat quality (G) in the landscape using a linear relationship given by $K_H(\mathrm{x}) = G(\mathrm{x})K_{H0}$, where K_{H0} is the maximum carrying capacity of hosts of type H in the environment (/km^2). We assume that all hosts are born susceptible to infection, and their per capita birth rate is b_H. Hosts die at a per capita rate d_H whether they are infected or not.

Infection dynamics. Tick infection with *B. burgdorferi* sensu stricto occurs when immature ticks successfully acquire the pathogen from an infected reservoir host following a blood meal, and we assume that pathogen acquisition is frequency-dependent (i.e., it depends on the proportion of infected hosts). Susceptible reservoir hosts become infected when they are bitten by an infected tick. The three forces of infection ($\lambda_T, \lambda_A,$ and λ_D) have the following form:

Ticks:

$$\lambda_T = \alpha_{TA}\beta_{A\to T}\left(\frac{I_A}{N_A+N_D+N_R}\right) + \alpha_{TD}\beta_{D\to T}\left(\frac{I_D}{N_A+N_D+N_R}\right),$$

Pathogen amplification hosts:

$$\lambda_A = \alpha_{TA}\beta_{T\to A}\left(\frac{I_T}{N_A + N_D + N_R}\right),$$

Pathogen dilution hosts:

$$\lambda_D = \alpha_{TD}\beta_{T\to D}\left(\frac{I_T}{N_A + N_D + N_R}\right).$$

The parameters α_{TA} and α_{TD} correspond to the daily rate at which immature ticks (whose number of individuals is given by $n_j N_T$, where n_j is the proportion of immature ticks) encounter pathogen amplification hosts A or pathogen dilution hosts D, respectively. The parameters $\beta_{A\to T}$ and $\beta_{D\to T}$ represent the probability that an immature tick acquires the pathogen from an infected amplification host or an infected dilution host, respectively. The parameters $\beta_{T\to A}$ and $\beta_{T\to D}$ define the probability that an infected tick transmits the pathogen to a susceptible amplification host or a susceptible dilution host, respectively.

Tick dispersal by hosts. Host movement is characterized by speed and turning frequency. The changes in host movement patterns in response to landscape heterogeneity are modeled through terms of diffusion $D_T(\mathrm{x},t)$ and advection $\overrightarrow{C_T}(\mathrm{x},t)$, in which the rates of diffusion η_T and advection ε_T vary according to three activity periods of migratory birds where ticks are active. These periods include bird migration to the north in spring, bird breeding during spring and summer, and bird migration to the south in late summer and autumn. For the northward and southward migration periods, the diffusion and advection rates were defined from movement parameters of migratory birds, whereas for the bird breeding season, the rates were calculated from movement parameters of terrestrial hosts. Tick dispersal by birds among resource-rich areas during the migration periods is thus thought to occur over long distances and to be more directed towards the north or south, whereas during the breeding season, ticks would be transported over short distances with more diffusive movement patterns of terrestrial hosts within resource-rich areas. Each bird activity period lasts 90 days, which gives a total period of 270 days per year during which birds disperse ticks. The diffusion term $D_T(\mathrm{x},t)$ defines random movement of ticks by hosts in the landscape, and the advection term $\overrightarrow{C_T}(\mathrm{x},t)$ describes directed movement of ticks by hosts towards the north or south of the landscape. The movement length is modeled following an exponentially decreasing function of habitat quality G to represent the tendency for hosts to move slowly and spend more time in resource-rich areas (Moorcroft and Lewis, 2006). The diffusion and advection terms have the following form:

$$D_T(\mathrm{x},t) = e^{-\omega_G G(\mathrm{x})}\eta_T,$$

$$\overrightarrow{C_T}(\mathrm{x},t) = e^{-\omega_G G(\mathrm{x})}\left(\frac{\hat{\mathrm{v}}}{\| \hat{\mathrm{v}} \|}\right)\varepsilon_T, \text{ with } \hat{\mathrm{v}} = \psi_T \overrightarrow{\mathrm{x}}_T + (1-\psi_T)\frac{\nabla G(\mathrm{x})}{\| \nabla G(\mathrm{x}) \|}.$$

The parameter ω_G describes the sensitivity to resource-rich areas, the parameter ψ_T defines the proportion of ticks moving northward and southward according to the bird activity period, and $\overrightarrow{\mathrm{x}}_T$ is a unit vector directed from $\mathrm{x} = (x,y)$ towards the north or south. The magnitude of the direction vector $\hat{\mathrm{v}}$ is measured by its Euclidean norm (represented by $\| \ \|$).

2.2. Model updates

We modified the original model by incorporating a temperature-dependent function for tick mortality in the population. Specifically, we varied the daily per capita mortality rate of ticks (d_T) as a function of annual cumulative degree-days above 0 °C (CDD > 0 °C), such that lower values of CDD > 0 °C (i.e., colder climate) are associated with higher daily per capita mortality rates. This relationship is a simplification of the main impact of temperature on tick population survival, and represents an indirect effect on overall mortality via the effects of temperature on interstadial development rates, and thus on life cycle length and the probability that ticks complete their life cycle (Ogden et al., 2005; Sagurova et al., 2019). The parameter d_T was defined using two metrics described in previous studies (Ludwig et al., 2016; Ogden et al., 2005): i) the time delay of each life cycle stage (including those that are dependent on temperature: pre-eclosion period of eggs, engorged larva to nymph development, engorged nymph to adult development, and pre-oviposition period of adult females; and those that are likely temperature-independent: post-eclosion or post-molting hardening period, period of feeding on hosts, and oviposition period of adult females), and ii) the fixed daily per capita mortality rate of ticks associated with each life cycle stage. From maps of average temperature weighted by the number of tick activity days per month, we calculated d_T by multiplying the two metrics described above (the details are given in Appendix A). We fitted a biexponential equation (Fig. 1) to the relationship between d_T and annual CDD > 0 °C for each tick species using a

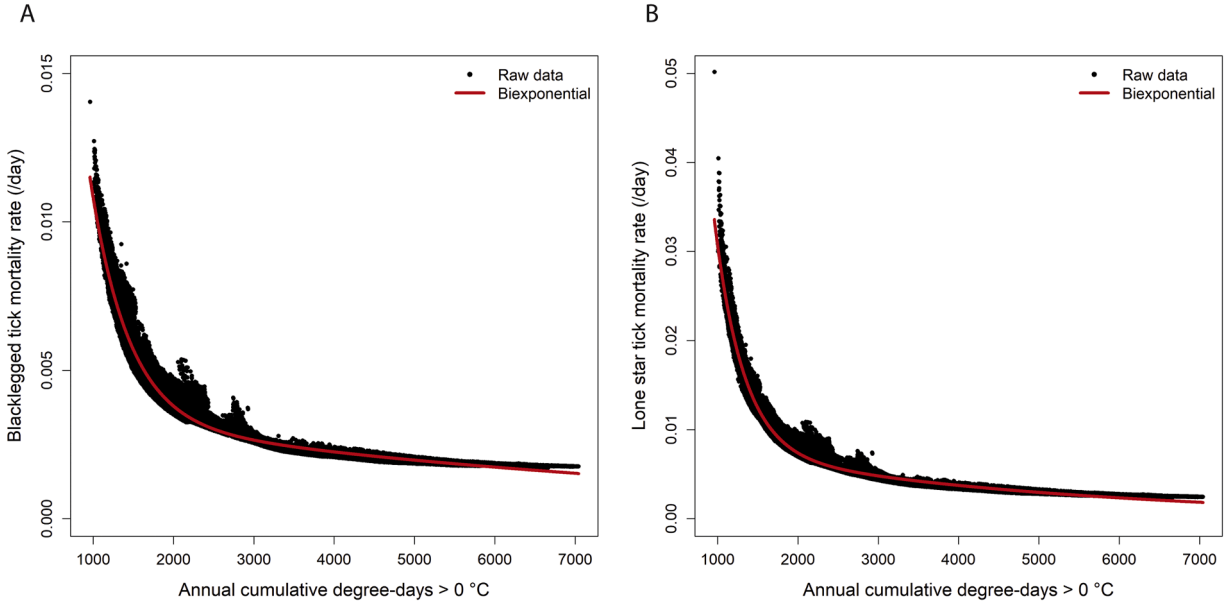

Fig. 1. Relationship between the daily per capita mortality rate of ticks and annual cumulative degree-days above 0°C. A biexponential equation was fitted to raw data for the blacklegged tick (*Ixodes scapularis*) (A) and the lone star tick (*Amblyomma americanum*) (B).

Table 1
Description of input parameters that are included in the reaction-advection-diffusion model. The model was parameterized for the blacklegged tick (*Ixodes scapularis*; IS), the causative bacterium of Lyme disease, *Borrelia burgdorferi* sensu stricto, and the lone star tick (*Amblyomma americanum*; AA). We also parameterized the model for different host species: the white-footed mouse (*Peromyscus leucopus*), the white-tailed deer (*Odocoileus virginianus*), and passerine birds including the American robin (*Turdus migratorius*), the ovenbird (*Seiurus aurocapilla*), the veery (*Catharus fuscescens*), and the wood thrush (*Hylocichla mustelina*). In the model, white-footed mice were considered as pathogen amplification hosts, white-tailed deer represented tick reproduction hosts, and passerine birds served as pathogen dilution hosts.

Symbol	Description	Range for the calibration analysis	Range for the sensitivity analysis	Value used for the scenarios	References/Comments
Category: infection dynamics					
α_{TA0}	Base rate at which immature ticks encounter amplification hosts (/day)	IS and AA: [0.00001 – 0.003]	IS: [0.0002 – 0.0029]	IS: 0.0016 AA: 0.0015	(Tardy et al., 2021)
α_{TD0}	Base rate at which immature ticks encounter dilution hosts (/day)	IS and AA: [0.000005 – 0.003]	IS: [0.0001 – 0.0029]	IS: 0.0016 AA: 0.0014	(Tardy et al., 2021)
α_{TA}	Rate at which immature ticks encounter amplification hosts (/day)	–	–	–	$\alpha_{TA0}N_A(\mathrm{x},t)^{0.515}n_j$, where $N_A(\mathrm{x},t)$ is the total density of amplification hosts at spatial location $\mathrm{x}=(x,y)$ at time t, and n_j is the proportion of immature ticks in the environment (Hartfield et al., 2011; Mount et al., 1997) $n_j = 1 - n_a$
α_{TD}	Rate at which immature ticks encounter dilution hosts (/day)	–	–	–	$\alpha_{TD0}N_D(\mathrm{x},t)^{0.515}n_j$, where $N_D(\mathrm{x},t)$ is the total density of dilution hosts at spatial location $\mathrm{x}=(x,y)$ at time t, and n_j is the proportion of immature ticks in the environment (Hartfield et al., 2011; Mount et al., 1997) $n_j = 1 - n_a$
$\beta_{A\to T}$	Probability that an infected amplification host transmits the pathogen to a susceptible tick (0 – 1)	IS: 0.92	IS: [0.6 – 0.99]	IS: 0.92	(LoGiudice et al., 2003)
$\beta_{D\to T}$	Probability that an infected dilution host transmits the pathogen to a susceptible tick (0 – 1)	IS: 0.12	IS: [0.08 – 0.2]	IS: 0.12	(LoGiudice et al., 2003)
$\beta_{T\to A}$	Probability that an infected tick transmits the pathogen to a susceptible amplification host (0 – 1)	IS: 0.83	IS: [0.6 – 0.99]	IS: 0.83	(Davis and Bent, 2011)
$\beta_{T\to D}$	Probability that an infected tick transmits the pathogen to a susceptible dilution host (0 – 1)	IS: 0.83	IS: [0.6 – 0.99]	IS: 0.83	(Davis and Bent, 2011; Tardy et al., 2021)
Category: host population dynamics					
b_A	Birth rate of amplification hosts (/day)	IS and AA: 0.02	IS: [0.014 – 0.026]	IS and AA: 0.02	(Wolff, 1985)
b_D	Birth rate of dilution hosts (/day)	IS and AA: 0.02	IS: [0.014 – 0.026]	IS and AA: 0.02	(Rodewald, 2015)
b_R	Birth rate of reproduction hosts (/day)	IS and AA: 0.01	IS: [0.007 – 0.013]	IS and AA: 0.01	(Green et al., 2017)
d_A	Natural mortality rate of amplification hosts (/day)	IS and AA: 0.01	IS: [0.007 – 0.013]	IS and AA: 0.01	(Collins and Kays, 2014)
d_D	Natural mortality rate of dilution hosts (/day)	IS and AA: 0.001	IS: [0.0007 – 0.0013]	IS and AA: 0.001	(Rodewald, 2015)
d_R	Natural mortality rate of reproduction hosts (/day)	IS and AA: 0.001	IS: [0.0007 – 0.0013]	IS and AA: 0.001	(Nelson and Mech, 1986)
r_A	Maximum per capita growth rate of amplification hosts (/day)	–	–	–	$b_A - d_A$
r_D	Maximum per capita growth rate of dilution hosts (/day)	–	–	–	$b_D - d_D$
r_R	Maximum per capita growth rate of reproduction hosts (/day)	–	–	–	$b_R - d_R$
K_{A0}	Maximum carrying capacity of amplification hosts ($/\mathrm{km}^2$)	IS and AA: 4000	IS: [2800 – 5200]	IS and AA: 4000	(Keesing et al., 2009)
K_{D0}	Maximum carrying capacity of dilution hosts ($/\mathrm{km}^2$)	IS and AA: 3200	IS: [2240 – 4160]	IS and AA: 3200	(LoGiudice et al., 2003)
K_{R0}	Maximum carrying capacity of reproduction hosts ($/\mathrm{km}^2$)	IS and AA: 50	IS: [35 – 65]	IS and AA: 50	(Rand et al., 2003)
K_A	Carrying capacity of amplification hosts ($/\mathrm{km}^2$)	–	–	–	$G(\mathrm{x})K_{A0}$, $G(\mathrm{x})$ represents the value of habitat suitability (or habitat quality) for hosts at spatial location $\mathrm{x}=(x,y)$
K_D	Carrying capacity of dilution hosts ($/\mathrm{km}^2$)	–	–	–	$G(\mathrm{x})K_{D0}$, $G(\mathrm{x})$ represents the value of habitat suitability (or habitat quality) for hosts at spatial location $\mathrm{x}=(x,y)$
K_R	Carrying capacity of reproduction hosts ($/\mathrm{km}^2$)	–	–	–	$G(\mathrm{x})K_{R0}$, $G(\mathrm{x})$ represents the value of habitat suitability (or habitat quality) for hosts at spatial location $\mathrm{x}=(x,y)$
Category: tick population dynamics					

(*continued on next page*)

Table 1 (*continued*)

Category: host population dynamics					
n_a	Proportion of adult ticks in the environment (0 – 1)	IS: 0.03 AA: 0.04	IS: [0.02 – 0.04]	IS: 0.03 AA: 0.04	(Daniels et al., 2000; Mangan et al., 2018)
α_{TR0}	Base rate at which adult ticks encounter reproduction hosts (/day)	IS and AA: [0.004 – 3]	IS: [0.1273 – 2.9438]	IS: 2.4321 AA: 2.4	(Tardy et al., 2021)
α_{TR}	Rate at which adult ticks encounter reproduction hosts (/day)	–	–	–	$\alpha_{TR0}N_R(\mathrm{x},t)^{0.515}n_a$, where $N_R(\mathrm{x},t)$ is the total density of reproduction hosts at spatial location $\mathrm{x}=(x,y)$ at time t (Hartfield et al., 2011; Mount et al., 1997)
B_T	Number of eggs produced per fed adult female tick (/day)	IS: 11 AA: 22	IS: [8 – 14]	IS: 11 AA: 22	(Ludwig et al., 2016; Mount et al., 1997)
n_{TR}	Number of ticks attached to a reproduction host (/day)	IS: 200 AA: 2000	IS: [140 – 260]	IS: 200 AA: 2000	(Bloemer et al., 1988; Madhav et al., 2004)
K_{T+}	Carrying capacity of ticks $(/\mathrm{km}^2)$	–	–	–	$n_{TR}K_R$ (Tardy et al., 2021)
θ_{T+}	Mate-finding Allee effect threshold (0 – 1)	IS and AA: [0.01 – 0.5]	IS: [0.0244 – 0.4876]	IS: 0.1150 AA: 0.0535	(Tardy et al., 2021)
K_{T-}	Tick density below which tick population growth becomes negative $(/\mathrm{km}^2)$	–	–	–	$\theta_{T+}K_{T+}$ (Hilker et al., 2007)
E_1	Multiplier of the first exponential of the temperature-dependent mortality function	IS: 0.062210 AA: 0.37780	IS: 0.062210	IS: 0.062210 AA: 0.37780	See Appendix A
E_2	Multiplier of the second exponential of the temperature-dependent mortality function	IS: 0.003708 AA: 0.00953	IS: 0.003708	IS: 0.003708 AA: 0.00953	See Appendix A
L_1	Natural logarithm of the rate constant of the first exponential of the temperature-dependent mortality function	IS: −6.160992 AA: −5.88138	IS: −6.160992	IS: −6.160992 AA: −5.88138	See Appendix A
L_2	Natural logarithm of the rate constant of the second exponential of the temperature-dependent mortality function	IS: −8.973773 AA: −8.35611	IS: −8.973773	IS: −8.973773 AA: −8.35611	See Appendix A
d_T	Temperature-dependent mortality rate of ticks (/day)	–	–	–	$E_1\exp(-\exp(L_1)\mathrm{CDD}>0^{\circ}\mathrm{C})+$ $E_2\exp(-\exp(L_2)\mathrm{CDD}>0^{\circ}\mathrm{C})$ See Appendix A
Category: host movement					
$\vec{\mathrm{x}}_T$	Unit vector directed from $\mathrm{x}=(x,y)$ towards the north or south	IS and AA: 1; 0; −1	IS: 1; 0; −1	IS and AA: 1; 0; −1	The parameter varies with the activity periods of migratory birds as follows: $\vec{\mathrm{x}}_T=\begin{cases}1 & \text{if } t>0 \;\&\; t\le 90\\ 0 & \text{if } t>90 \;\&\; t\le 180\\ -1 & \text{if } t>180 \;\&\; t\le 270\end{cases}$, where t is time (Tardy et al., 2021)
ψ_{Tn}	Weighting factor that controls the proportion of ticks moving to the north by migratory birds (0 – 1)	IS and AA: [0.01 – 1]	IS: [0.1396 – 0.9830]	IS: 0.7606 AA: 0.6384	(Tardy et al., 2021)
ψ_{Ts}	Weighting factor that controls the proportion of ticks moving to the south by migratory birds (0 – 1)	IS and AA: [0 – 0.5]	IS: [0.0232 – 0.4716]	IS: 0.1402 AA: 0.3166	(Tardy et al., 2021)
ψ_T	Weighting factor that controls the proportion of ticks moving to the north and south by migratory birds (0 – 1)	–	–	–	The parameter varies with the activity periods of migratory birds as follows: $\psi_T=\begin{cases}\psi_{Tn} & \text{if } t>0 \;\&\; t\le 90\\ 0 & \text{if } t>90 \;\&\; t\le 180\\ \psi_{Ts} & \text{if } t>180 \;\&\; t\le 270\end{cases}$, where t is time
ρ_D	Distance moved by migratory birds per day (km)	IS and AA: [40 – 130]	IS: [41.9314 – 127.8678]	IS: 110.0392 AA: 73.7431	(Tardy et al., 2021)
ρ_H	Distance moved by terrestrial hosts per day (km)	IS and AA: [0.1 – 1]	IS: [0.1737 – 0.9849]	IS: 0.6064 AA: 0.8166	(Tardy et al., 2021)
κ_D	Concentration parameter of the von Mises distribution describing the magnitude of directional bias towards the north or south for migratory birds	IS and AA: [0.01 – 2]	IS: [0.0674 – 1.8670]	IS: 0.5469 AA: 0.6364	(Tardy et al., 2021)
κ_H	Concentration parameter of the von Mises distribution describing the magnitude of directional bias towards the north or south for terrestrial hosts	IS and AA: [0 – 0.5]	IS: [0.0024 – 0.2222]	IS: 0.0207 AA: 0.0950	(Tardy et al., 2021)
Δ_{fT}	Duration of tick feeding on migratory birds and terrestrial hosts (days)	IS and AA: 5	IS: [3 – 7]	IS and AA: 5	(Ludwig et al., 2016; Ogden et al., 2005, 2008b)
ρ_{TD}	Distance moved by ticks on migratory birds per day (km)	–	–	–	$\frac{\Delta_{fT}}{\Delta_{Dm}}[\rho_D\psi_T+\rho_H(1-\psi_T)]$, where Δ_{Dm} is the duration of northward or southward migration of birds (days) $\Delta_{Dm}=90$ days
ρ_{TH}	Distance moved by ticks on terrestrial hosts per day (km)	–	–	–	$\frac{\Delta_{fT}\rho_H}{\Delta_{Db}}$, where Δ_{Db} is the duration of bird breeding season (days) $\Delta_{Db}=90$ days

(*continued on next page*)

Table 1 (*continued*)

Category: host population dynamics					
η_{TD}	Diffusion rate of ticks by migratory birds (km^2/day)	–	–	–	$\frac{\rho_{TD}{}^2}{2\tau}$, where τ is the time unit (Moorcroft and Lewis, 2006) $\tau = 1$ day
η_{TH}	Diffusion rate of ticks by terrestrial hosts (km^2/day)	–	–	–	$\frac{\rho_{TH}{}^2}{2\tau}$, where τ is the time unit (Moorcroft and Lewis, 2006) $\tau = 1$ day
η_T	Diffusion rate of ticks by migratory birds and terrestrial hosts (km^2/day)	–	–	–	The parameter varies with the activity periods of migratory birds as follows: $\eta_T = \begin{cases} \eta_{TD} & \text{if } t > 0 \ \& \ t \leq 90 \\ \eta_{TH} & \text{if } t > 90 \ \& \ t \leq 180 \\ \eta_{TD} & \text{if } t > 180 \ \& \ t \leq 270 \end{cases}$, where t is time
ε_{TD}	Advection rate of ticks by migratory birds (km/day)	–	–	–	$\frac{\kappa_D \rho_{TD}}{2\tau}$, where τ is the time unit (Moorcroft and Lewis, 2006) $\tau = 1$ day
ε_{TH}	Advection rate of ticks by terrestrial hosts (km/day)	–	–	–	$\frac{\kappa_H \rho_{TH}}{2\tau}$, where τ is the time unit (Moorcroft and Lewis, 2006) $\tau = 1$ day
ε_T	Advection rate of ticks by migratory birds and terrestrial hosts (km/day)	–	–	–	The parameter varies with the activity periods of migratory birds as follows: $\varepsilon_T = \begin{cases} \varepsilon_{TD} & \text{if } t > 0 \ \& \ t \leq 90 \\ \varepsilon_{TH} & \text{if } t > 90 \ \& \ t \leq 180 \\ \varepsilon_{TD} & \text{if } t > 180 \ \& \ t \leq 270 \end{cases}$, where t is time
σ_G	Rate which the daily distance moved by ticks on migratory birds and terrestrial hosts decreases with increasing resource availability	IS and AA: [0.1 – 10]	IS: [0.9221 – 9.7933]	IS: 0.9224 AA: 4.3968	(Tardy et al., 2021)
ω_G	Sensitivity (or attraction) to areas of high resource availability	–	–	–	$2\sigma_G$ (Moorcroft and Lewis, 2006)
Category: landscape					
α_G	Inflection point of the habitat suitability function	IS and AA: −1.5; −3; −4; −5.5	IS: −1.5; −3; −4; −5.5	IS: −1.5 AA: −1.5	See Section 2.2
β_G	Slope at the inflection point of the habitat suitability function	IS and AA: 28	IS: 28	IS: 28 AA: 28	See Section 2.2
ϕ_G	Forest proportion threshold delineating suitable habitat for hosts (0 – 1)	IS and AA: 0.05; 0.1; 0.15; 0.2	IS: 0.05; 0.1; 0.15; 0.2	IS: 0.05 AA: 0.05	Each value is given by a combination of α_G and β_G: (−1.5; 28), (−3; 28), (−4; 28) and (−5.5; 28) give ϕ_G= 0.05, ϕ_G= 0.1, ϕ_G= 0.15 and ϕ_G= 0.2, respectively
Category: temperature					
ST_{DD}	Degree-day threshold for tick population survival	IS: [2400 – 3300] AA: [2600 – 3500]	IS: [2422 – 3274]	IS: 2679 AA: 2827	(Ogden et al., 2005; Sagurova et al., 2019; Wu et al., 2013)
I_{DD}	Increasing value of degree-days	IS and AA: 0	IS: [0 – 600]	IS and AA: 0; 100; 200; 400; 600	Environment and Climate Change Canada [‡]; National Oceanic and Atmospheric Administration [‡]; ClimateNA [‡]

[‡] The uncertainty range of the input parameter I_{DD} was adjusted to represent the global increasing trend of degree-days captured from annual climate data recorded at 2047 meteorological stations in North America during the periods of 1981 – 2010 and 1991 – 2020. The station locations were provided by Environment and Climate Change Canada (ECCC; data available at https://climate.weather.gc.ca/climate_normals/), and National Oceanic and Atmospheric Administration (NOAA; data available at https://www.ncdc.noaa.gov/cdo-web/datatools/normals). We used the ClimateNA software package (version 7.00; data available at http://climatena.ca/) to obtain the climate data.

nonlinear least-squares regression to estimate each of the equation parameters. The biexponential equation has the following form:

$$d_T(\mathrm{CDD} > 0^{\circ}\mathrm{C}) = E_1 \exp(-\exp(L_1)\mathrm{CDD} > 0^{\circ}\mathrm{C}) + E_2 \exp(-\exp(L_2)\mathrm{CDD} > 0^{\circ}\mathrm{C})$$

The parameters E_1 and E_2 represent the multiplier of the first and second exponential, respectively. The parameters L_1 and L_2 represent the natural logarithm of the rate constant of the first and second exponential, respectively. We chose a biexponential equation rather than an exponential decay equation because the biexponential equation has greater flexibility and showed a better fit to the data, in particular for the distribution tails (Fig. A.2 in Appendix A). The parameter values are in Table 1. More details on the fitting procedure can be found in Appendix A.

Carrying capacities of hosts changed according to habitat quality in the landscape using a linear relationship as in Tardy et al. (2021). Habitat quality (G) was derived from a habitat suitability index that is bounded by the interval [0 – 1], and follows the following logistic form:

$$G = \frac{1}{1 + \exp(-\alpha_G - \beta_G p_{Forest})} \quad (1)$$

The parameter α_G represents the inflection point of the logistic function, β_G is the slope at the inflection point of the function, and p_{Forest} corresponds to the proportion of forest cover type. In general, forests can harbor a high diversity of host species, and are also highly suitable habitats for blacklegged ticks and lone star ticks (Allan et al., 2003; Ginsberg et al., 2020; Guerra et al., 2002). In this study, we tested different values for α_G ($\alpha_G = -1.5, -3, -4,$ and -5.5) while keeping the value of β_G constant ($\beta_G = 28$) (Fig. 2; see also Fig. B.1 in Appendix B for another representation of habitat suitability layers). For example, the combination of $\alpha_G = -1.5$ and $\beta_G = 28$ indicates that habitat cells with a

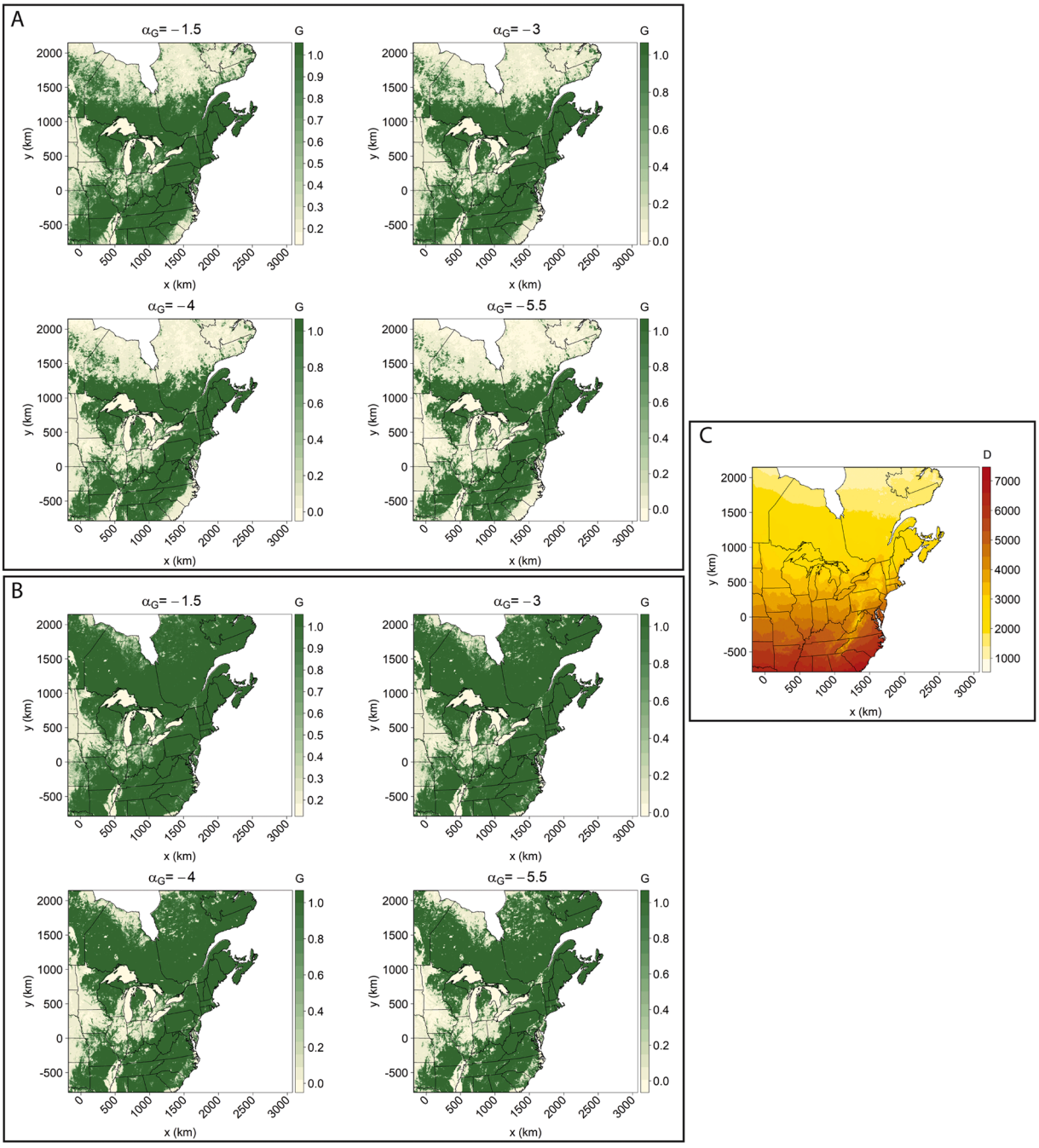

Fig. 2. Overview of data layers used as model inputs. The layers define habitat suitability $G(x)$ for hosts of the blacklegged tick (*Ixodes scapularis*) (A), habitat suitability $G(x)$ for hosts of the lone star tick (*Amblyomma americanum*) (B), and temperature suitability $D(x)$ for the two tick species (C), which was expressed in terms of annual cumulative degree-days above 0 °C. Different values for the inflection point of the habitat suitability function were tested ($\alpha_G = -1.5, -3, -4,$ and -5.5) while keeping the value for the slope at the inflection point of the function constant ($\beta_G = 28$). The dimension of each landscape is 2930 km × 3250 km with a cell resolution of 10 km.

forest proportion threshold (ϕ_G) of 0.05 are considered as suitable for hosts (i.e.,$G \geq 0.5$) (see Fig. B.2 in Appendix B).

2.3. Model parameterization

The model was parameterized from empirical and modeling studies, as well as expert opinion for two simulation experiments: (1) with *B. burgdorferi* sensu stricto and the blacklegged tick, and (2) with the lone star tick without infection dynamics. Given that there is no infection process in the lone star tick model, the changes in lone star tick population dynamics are mainly driven by tick reproduction hosts, which allows implicitly modeling dependence of this tick species on ungulates. In the lone star tick model, input parameters associated with the infection process were set to zero, and the density of infected ticks was not modeled. In the two experiments, we also parameterized the model for different host species similarly to Tardy et al. (2021): the white-footed mouse (*Peromyscus leucopus*), the white-tailed deer (*Odocoileus virginianus*), and passerine birds including the American robin (*Turdus migratorius*), the ovenbird (*Seiurus aurocapilla*), the veery (*Catharus fuscescens*), and the wood thrush (*Hylocichla mustelina*). In the model, white-footed mice were considered as pathogen amplification hosts, white-tailed deer represented tick reproduction hosts, and

passerine birds served as pathogen dilution hosts.

To perform the global sensitivity analysis (Objective 1), we defined uncertainty ranges for literature-derived known model input parameters by setting the minimum and maximum as 30% lesser and greater than their default values, whereas uncertainty ranges for input parameters that were considered as highly uncertain or unknown were defined from a calibration analysis (CA) as in Tardy et al. (2021). The CA for each tick species was based on an approximate Bayesian computation analysis using a simple rejection sampling method (see Appendix C for more details) because this method could produce lower prediction errors compared to regression-based correction methods using local linear regression and neural networks, in particular when the tolerance rates (i.e., the proportion of accepted simulations) decreased (Fig. C.1 in Appendix C). We used median estimates of the highly uncertain or unknown input parameters obtained with the CA to explore the possible consequences of increasing temperature on northward range expansion of ticks and tick-borne pathogens (Objective 2). In total, 1000 different combinations of 13 input parameters were sampled using Latin hypercube sampling, so that 1000 simulations were run to perform the CA. For the first experiment, the rate of global spread of infected blacklegged ticks (km/day) and blacklegged tick infection prevalence (0 – 1) were considered as model output variables in the CA. The observed summary statistics of these output variables were calculated as the mean of the minimum and maximum of a plausible value range that was derived from literature and expert opinion (Thiele et al., 2014). Similarly to our previous study (Tardy et al., 2021), the rate of spread by infected blacklegged ticks varied from 0.009 km/day to 0.2 km/day (Leighton et al., 2012; Simon et al., 2014), whereas blacklegged tick infection prevalence varied from 0 to 0.7 (Ogden et al., 2010). Such estimates are not available for the lone star tick. Consequently, an overall correct prediction rate (i.e., the proportion of correctly predicted occurrences) served as the output variable in the CA for the second experiment. This output variable was used for comparison of the model predictions with field observations of lone star ticks. The observed summary statistics of the output variable were based on an overall correct prediction rate of 100%. The field observations corresponded to lone star tick presence data (Lado et al., 2020) that came from the Ohio State Acarology Collection (OSAL), the United States National Tick Collection (USNTC), and records retrieved from Raghavan et al. (2019). After extracting uninfected lone star tick density predictions from our model for each presence observation, the density predictions were then converted to binary presence-absence predictions using four local tick establishment thresholds that were defined as 1%, 5%, 10%, and 20% of tick carrying capacity. In particular, a spatial location $\mathrm{x} = (x, y)$ is considered as infested with ticks if the tick population size at the location exceeds a given establishment threshold value among the four tested thresholds (Tardy et al., 2021).

To assess the capacity of the model to simulate northward range expansion of ticks and tick-borne pathogens with climate change (Objective 2), theoretical increases in temperature (I_{DD}) were selected to broadly represent the global increasing trend of degree-days captured from annual climate data recorded at 2047 meteorological stations in North America during the periods of 1981 – 2010 and 1991 – 2020. Data sources are detailed in Table 1. We tested the potential effects of increasing temperature scenarios by applying increases of 100, 200, 400 and 600 degree-days to baseline annual CDD > 0 °C (no increase). This approach is, of course, a simple sensitivity analysis and not a full exploration of possible effects of climate change on northward range expansion of ticks and tick-borne pathogens, which would require more detailed use of time- and location-specific projected outputs of climate models, and exploration of the range of realistic representative greenhouse gas concentration pathways linked to shared socioeconomic pathways.

2.4. Model inputs and outputs

The model was applied to the Canadian provinces of Manitoba, Ontario, Quebec, New Brunswick, Nova Scotia and Prince Edward Island, together with the eastern half of the United States (Fig. 2), where blacklegged tick and lone star tick populations are established or have been reported (Sonenshine, 2018). Model inputs were derived from publicly available landscape and climate data sources. For each tick species, we built one map of habitat suitability for hosts and one map of temperature suitability for ticks to assess the effects of landscape and increasing temperature changes on spread dynamics of ticks and tick-borne pathogens (Fig. 2). From a grid of 2930 km $\times$ 3250 km with a cell resolution of 10 km encompassing the study area, we calculated the proportion of forest cover within each cell, and we applied Eq. (1) to obtain the map of habitat suitability for hosts $G(\mathrm{x})$. The proportion of forest cover was obtained using the 2015 land cover dataset of the North American Land Change Monitoring System (NALCMS). This dataset is derived from 30-m Landsat satellite images and includes 19 land cover classes (data available at http://www.cec.org/north-american-land-change-monitoring-system/). For the blacklegged tick, the forest cover classes included deciduous and mixed forests, whereas we considered all forest cover types (i.e., deciduous, coniferous, and mixed) for the lone star tick. Empirical studies showed high survival of lone star ticks in both coniferous and deciduous forests (e.g., Ginsberg and Zhioua, 1996; Koch, 1984), suggesting that this tick species is a potential habitat generalist (Mathisson et al., 2021). On the contrary, the blacklegged tick has been found to be more abundant and have a better survival in deciduous forests than in coniferous forests (e.g., Guerra et al., 2002; Lindsay et al., 1999). Leaf litter depth and acorn production attracting white-tailed deer and white-footed mice are possible predictors that may explain this habitat association (Mathisson et al., 2021; McShea and Schwede, 1993; Ostfeld et al., 2001; Schulze et al., 1995). In addition, we calculated monthly degree-days above 0 °C using monthly mean temperature data from 1991 to 2020, which were generated from the ClimateNA software package (version 7.00). If the monthly mean temperature value was above 0 °C, the temperature value was multiplied by the number of days in the month (Clow et al., 2017). The values of monthly degree-days above 0 °C were then summed across the 12 months of the year to obtain annual CDD > 0 °C and used to build the map of temperature suitability for ticks $D(\mathrm{x})$. All data layers were reprojected to NAD 1983 Albers Equal Area Conic projection. Finally, the maps were discretized into a two-dimensional rectangular mesh of 95,225 bilinear quadrangular elements (325 cells in the x direction and 293 cells in the y direction). Each mesh node at spatial location $\mathrm{x} = (x, y)$ was characterized by a value of habitat suitability for hosts $G(\mathrm{x})$ and temperature suitability for ticks $D(\mathrm{x})$. The maps were created using the *rgdal, gstat, raster, sf, maptools* and *rgeos* packages (Bivand et al., 2022; Bivand and Lewin-Koh, 2022; Bivand and Rundel, 2021; Hijmans, 2022; Pebesma, 2018, 2004) in the R statistical software (version 4.1.2) (R Development Core Team, 2019).

Throughout the simulation experiments, the main model output was the spatial density pattern of ticks (infected or not) at the end of the simulation. For the baseline scenario, the extent of the spatial distribution of ticks was compared with field observations, and for the theoretical scenarios of increasing temperature, the extent of the distribution was compared with that of projected spatial distributions of ticks reported in the literature. Similarly to Tardy et al. (2021), the rate of global spread of infected blacklegged ticks or uninfected lone star ticks (km/day), blacklegged tick infection prevalence (0 – 1), and the maximum density of infected blacklegged ticks or uninfected lone star ticks (number of ticks/km^2) were also calculated at each time step of 10 days without significant loss of accuracy. These metrics were used to perform the calibration and sensitivity analyses.

2.5. Model initialization

A simulation was initialized either with uninfected blacklegged ticks that were located at two entry areas of 400 km^2 in the southern United States (one in Georgia and one in Texas), or with uninfected lone star ticks that were located at two entry areas of 400 km^2 in the southern United States (one in South Carolina and one in Texas). These initialization areas represent theoretical sites for origins of tick populations simply to begin simulations of northward range spread. The objective of this study was not to observe the spatial progress of the blacklegged tick and lone star tick invasion at each time step given that the model was not applied to plausible scenarios of climate, socioeconomic and land use/land cover changes. Using theoretical scenarios of increasing temperature, we instead evaluated the model's capacity to simulate the expected impact of climate warming on the northward range expansion of two tick species, as in other studies, at the end of the simulations. The entry areas contained a number of ticks equal to the carrying capacity K_T, and we assumed that 15% of blacklegged ticks were infected in the entry areas (Hengge et al., 2003). Amplification, dilution and reproduction host populations were distributed across the habitat suitability gradient $G(x)$ with a number of individuals equal to their carrying capacity K_A, K_D and K_R, respectively. The model time step was set to one day, and the model ran during the three activity periods of migratory birds where ticks are active (270 days over one year) for 50 years.

2.6. Sensitivity analysis

We performed a global sensitivity analysis (SA) to assess the sensitivity of the model to variations in input parameters. As in Tardy et al. (2021), the rate of spread by infected blacklegged ticks, blacklegged tick infection prevalence and the maximum density of infected blacklegged ticks were used as output variables. We selected 31 input parameters for the SA, including parameters associated with six categories according to their effect on ecological processes incorporated in the model: host movement, tick population dynamics, host population dynamics, infection dynamics, landscape, and temperature (Table 1). A Latin hypercube sampling design was used to sample 1200 different combinations of the 31 input parameters. Finally, we used boosted regression tree (BRT) models (Elith et al., 2008) to explore the relative contribution of the 31 input parameters to the output variables, and to identify the most influential input parameters similarly to our previous studies (Tardy et al., 2021, 2022). A Gaussian error structure was chosen for the loss function. The maximum density of infected blacklegged ticks was log-transformed in the BRT models to achieve a Gaussian error distribution and to stabilize the observation variance (Zuur et al., 2007). We tested several combinations of learning rate (0.01, 0.005, 0.001), tree complexity (1 – 5) and bag fraction (0.5, 0.7, 0.9) to define optimal settings for the BRT models, and we selected the parameter combination with the lowest 10-fold cross-validation deviance to fit the final BRT model. The relative influence of the six categories was also evaluated. We visualized the relationships between the output variables and the most influential input parameters using partial dependence plots in which 95% confidence intervals were obtained from 200 bootstrap replicates. The significance of the strongest interactions was tested using 100 bootstrap resampling iterations (Jouffray et al., 2019; Pinsky and Byler, 2015). We built the BRT models using the *dismo* and *ggBRT* packages (Hijmans et al., 2020; Jouffray et al., 2019) in the R statistical software (version 4.1.2) (R Development Core Team, 2019).

2.7. Model validation

We compared the simulated spatial distribution pattern of infected blacklegged ticks with field observations ($N = 96$) based on 2019 data of uninfected ($N = 48$) and *B. burgdorferi* sensu stricto-infected ($N = 26$) tick abundance (Guillot et al., 2020). We considered both uninfected and infected ticks sampled in the field to achieve a larger number of observations and to improve model validation performance. These data were collected from sentinel surveillance sites of the Canadian Lyme Sentinel Network (CaLSeN). For the validation analysis, we converted the empirical abundance data to presence (abundance > 0) or absence (abundance $= 0$) data. After extracting infected blacklegged tick density predictions from the model for each presence-absence location, the density predictions were then converted to binary presence-absence predictions using the four local tick establishment thresholds (i.e., 1%, 5%, 10%, and 20%). Finally, we calculated an overall correct prediction rate (i.e., the proportion of correctly predicted occurrences) to assess the model predictive power under the baseline scenario (no degree-day increase). Note that for the lone star tick, field observation data were used to estimate the "overall correct prediction rate" in the CA, but formal validation was not possible.

3. Results

3.1. Model performance

3.1.1. Model calibration and validation

The CA suggests that a landscape with areas of habitat suitability for hosts based on a deciduous and mixed forest proportion threshold of 0.05 yielded better calibrated predictions of infected blacklegged tick distribution patterns. For the lone star tick, the model predictions were better calibrated with habitat suitability areas based on a deciduous, coniferous and mixed forest proportion threshold of 0.05. The predicted baseline spatial patterns of infected blacklegged tick and uninfected lone star tick densities were highly correlated with the habitat suitability patterns of hosts (Spearman rank correlation coefficient for the blacklegged tick: $r = 0.61$, $p < 0.05$; Spearman rank correlation coefficient for the lone star tick: $r = 0.65$, $p < 0.05$). Regarding the model validation, the comparison of the baseline model predictions with the field observations suggests that the model performed well when predicting the spatial distribution of infected blacklegged ticks in the landscape, with an overall correct prediction rate of 92%, 92%, 90% and 85% for the tick establishment threshold of 1%, 5%, 10% and 20%, respectively.

3.1.2. Sensitivity analysis

Regardless of the tick establishment thresholds, the BRT models revealed that two input parameters were the most influential predictors of the rate of spread by infected blacklegged ticks. The first strongest predictor was a negative nonlinear relationship with the rate at which the daily distance moved by blacklegged ticks on migratory birds and terrestrial hosts decreases with increasing resource availability (σ_G; relative influence of 35%, 44%, 42% and 40% with a tick establishment threshold of 1%, 5%, 10% and 20%, respectively; Fig. D.1 and Fig. D.3 in Appendix D). This input parameter controls the attraction of migratory birds and terrestrial hosts to resource-rich areas. The second strongest predictor was a negative nonlinear relationship with the mate-finding Allee effect threshold (θ_{T+}; relative influence of 16%, 17%, 14% and 16% with a tick establishment threshold of 1%, 5%, 10% and 20%, respectively; Fig. D.1 and Fig. D.3 in Appendix D). Blacklegged tick infection prevalence was highly sensitive to the base rate at which immature blacklegged ticks encounter pathogen amplification hosts (α_{TA0}; 38% relative influence, positively correlated; Fig. D.2 and Fig. D.4 in Appendix D) and the base rate at which adult blacklegged ticks encounter tick reproduction hosts (α_{TR0}; 32% relative influence, negatively correlated; Fig. D.2 and Fig. D.4 in Appendix D). Finally, three input parameters contributed most strongly to predicting maximum density of infected blacklegged ticks: the base reproduction host-finding rate (α_{TR0}; 29% relative influence, negatively correlated; Fig. D.2 and Fig. D.4 in Appendix D), the base amplification host-finding rate (α_{TA0}; 22% relative influence, positively correlated; Fig. D.2 and Fig. D.4 in Appendix D), and the blacklegged tick burden on reproduction hosts (n_{TR}; 10% relative influence, positively correlated; Fig. D.2 and Fig. D.4 in Appendix D). A summary of predictive performance of each BRT

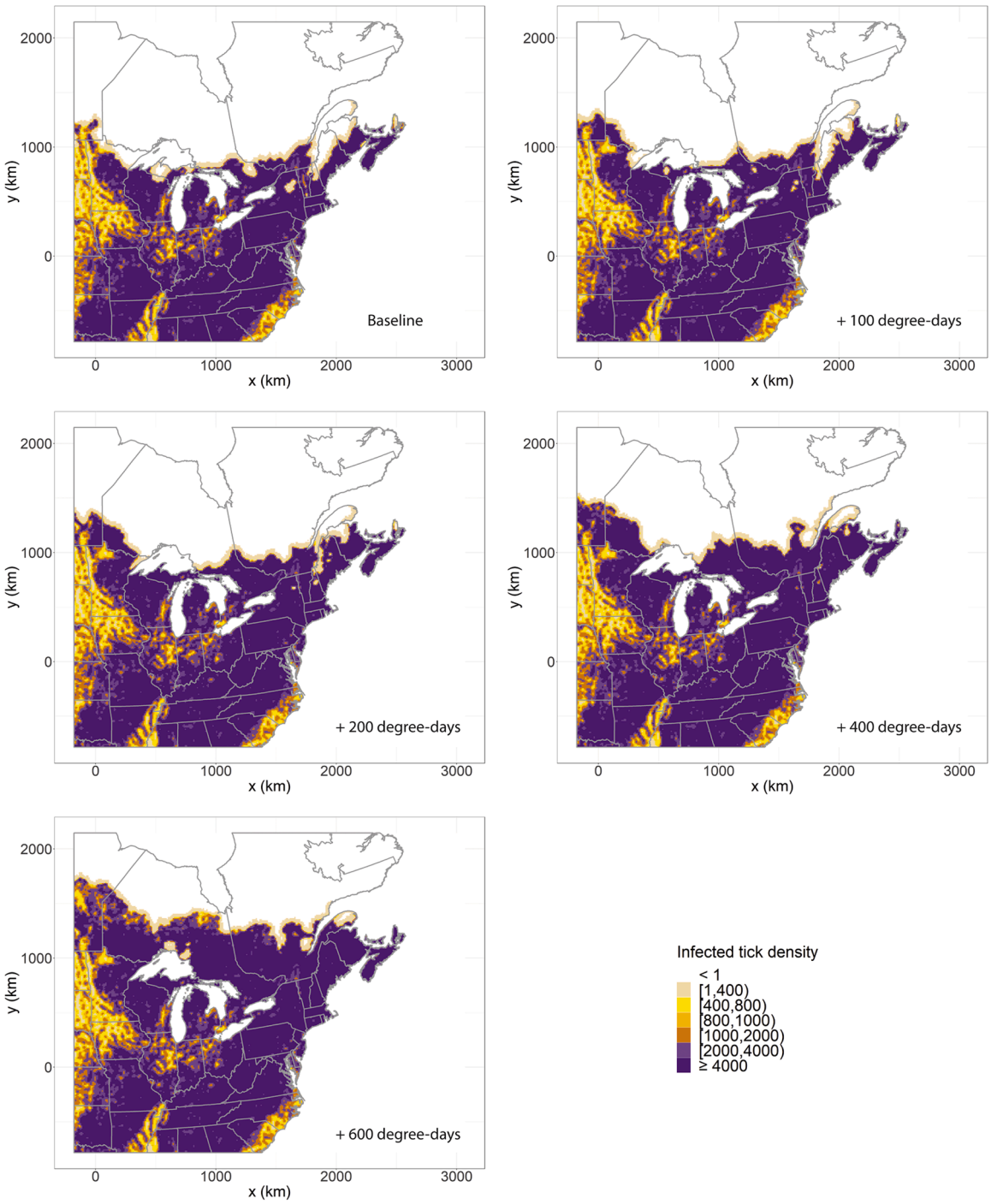

Fig. 3. Effects of increasing temperature on the spatial distribution of *Borrelia burgdorferi* sensu stricto-infected blacklegged ticks (*Ixodes scapularis*). Temperature was expressed in terms of annual cumulative degree-days above 0 °C (CDD > 0 °C). The potential effects of increasing temperature scenarios were tested by applying increases of 100, 200, 400 and 600 degree-days to baseline annual CDD > 0 °C (no increase).

model and the relative influence of six categories characterizing the input parameters can be found in Appendix D (Table D.1 and Table D.2, respectively). The most influential input parameters on all model output variables were among those identified by the global SA of the original model (Tardy et al., 2021).

3.2. *Effects of increasing temperature on range expansion of ticks and tick-borne pathogens*

An increase of up to 600 degree-days above baseline annual CDD > 0 °C resulted in expansion of the spatial distribution of infected blacklegged ticks and uninfected lone star ticks into higher latitudinal regions in different ways (Fig. 3 and Fig. 4). Compared to the baseline scenario (no degree-day increase), an increase of 100, 200, 400 and 600 degree-days increased the extent of the baseline spatial distribution of infected blacklegged ticks by 4.4%, 7.8%, 17% and 31%, respectively, whereas the extent of the baseline spatial distribution of uninfected lone star ticks increased by 0.6%, 0.8%, 0.7% and 0.7%, respectively. The speed of the northward invasion of blacklegged ticks was more sensitive to increasing temperature than that of lone star ticks, with a speed reaching

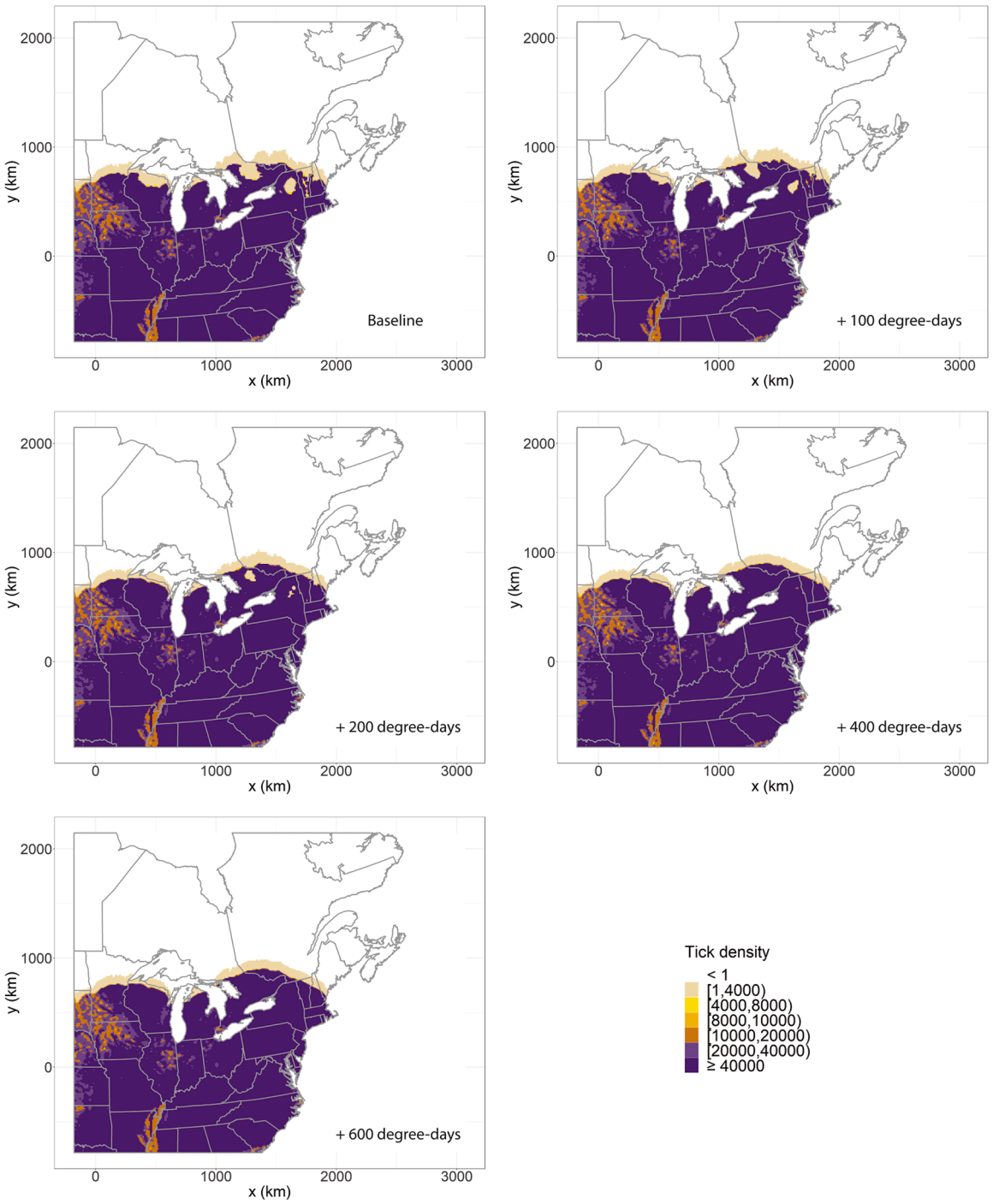

Fig. 4. Effects of increasing temperature on the spatial distribution of uninfected lone star ticks (*Amblyomma americanum*). Temperature was expressed in terms of annual cumulative degree-days above 0 °C (CDD > 0 °C). The potential effects of increasing temperature scenarios were tested by applying increases of 100, 200, 400 and 600 degree-days to baseline annual CDD > 0 °C (no increase).

61 km/year (range: 31 – 96 km/year) for the blacklegged tick and 23 km/year (range: 18 – 26 km/year) for the lone star tick under the + 600 degree-days scenario (Table 2). These differences in the extent of areas infested with blacklegged ticks and lone star ticks, as well as in the speed of range expansion, were explained by contrasting calibrated values of the input parameter controlling the attraction of migratory birds and terrestrial hosts to resource-rich areas (σ_G= 0.9 for the blacklegged tick and σ_G= 4.4 for the lone star tick). For migratory birds carrying lone star ticks, increasing resource availability resulted in a more rapid decrease of their distance traveled each day compared to birds carrying blacklegged ticks.

4. Discussion

In this study, we explored a "reaction-advection-diffusion" type model based on partial differential equations as a tool that may be used to predict northward range expansion of ticks and tick-borne pathogens with climate change. The model integrates a mechanistic formulation of host movement, and is designed to simulate both long-distance dispersal of migratory birds at the continental scale and local-scale movement of terrestrial hosts. We applied the model to two tick species of high veterinary and medical importance in North America, the blacklegged tick and the lone star tick, by considering theoretical scenarios of increasing

Table 2
Predicted speed (km/year) of the northward invasion of *Borrelia burgdorferi* sensu stricto-infected blacklegged ticks (*Ixodes scapularis*) and uninfected lone star ticks (*Amblyomma americanum*) under increasing temperature scenarios (i.e., increases of 100, 200, 400 and 600 degree-days to baseline annual cumulative degree-days above 0 °C).

	Tick establishment threshold							
	***B. burgdorferi* sensu stricto-infected blacklegged tick**				**Uninfected lone star tick**			
Scenario	**1%**	**5%**	**10%**	**20%**	**1%**	**5%**	**10%**	**20%**
Baseline	83.96	60.07	37.50	24.03	24.74	25.54	22.92	16.94
+ 100 degree-days	86.32	61.91	39.19	25.23	24.93	25.76	23.13	17.23
+ 200 degree-days	87.43	63.14	40.46	26.24	25.20	26.06	23.31	17.39
+ 400 degree-days	90.31	65.45	42.86	28.14	25.43	26.25	23.47	17.54
+ 600 degree-days	96.28	70.37	47.31	31.04	25.45	26.25	23.49	17.56

temperature (i.e., increases of 100, 200, 400 and 600 degree-days to baseline annual CDD > 0 °C) throughout eastern North America. The simulation experiments of this study indicate that the model is capable of simulating the expected impact of climate warming on range spread of the blacklegged tick and, to a lesser extent, the lone star tick, as in other studies (e.g., McPherson et al., 2017; Sagurova et al., 2019). However, predictions about future spatial distributions of ticks and tick-borne pathogens require both the use of model outputs under appropriate scenarios of climate, socioeconomic and land use/land cover changes, as well as simulations on long time scales.

4.1. Model performance

Similar to our previous study (Tardy et al., 2021), the global SA shows that the attraction of migratory birds to resource-rich areas during their northward migration in spring and the mate-finding Allee effect in tick population dynamics play a dominating role in the speed of the northward invasion of blacklegged ticks infected by *B. burgdorferi* sensu stricto, which points to the importance of considering these two ecological drivers in predicting distribution patterns of ticks and their pathogens in heterogeneous landscapes. Among billions of birds moving annually between wintering sites and breeding sites around the world (Berthold, 2001), most long-distance migrating passerines accomplish intermittent flights with stopovers to feed and rest before their next flight (Alerstam, 1993). Because stopover duration strongly influences the speed of migration (Schaub and Jenni, 2001), stopover behavior is a key determinant of the speed of northward invasion of infected ticks (Tardy et al., 2021). In our simulation results, high rates of infected blacklegged tick spread were associated with low attractiveness of rich-resource areas along the northward axis, which corroborates the findings of our previous study (Tardy et al., 2021). We also found that a low critical threshold of blacklegged tick density (< 25% of tick carrying capacity) determined by the mate-finding Allee effect contributed to increased rates of infected blacklegged tick spread. This suggests that manipulation of mate-finding Allee effects could be exploited to limit infected blacklegged tick invasion through the use of control methods that disrupt the tick mating process, including pheromone-based methods (Sonenshine, 2006) and application of acaricides to tick reproduction hosts (such as deer) (Stafford III and Williams, 2017).

Considering the veterinary and public health significance of blacklegged ticks and lone star ticks, predicting their spatial distribution under current and future climatic change scenarios is needed to provide insight into potential distributional shifts or expansions into higher elevations and altitudes (Gilbert, 2021; Ogden et al., 2021). In general, we achieved satisfactory model performance, suggesting that the model may be used as a tool to predict future range expansion of these two tick species. The baseline distribution areas of blacklegged ticks infected by *B. burgdorferi* sensu stricto estimated in this study covered the majority of climatically suitable areas of the southern Canada (including the provinces of Manitoba, Ontario, Quebec, New Brunswick, and Nova Scotia) under the projected climate conditions for the 2011–2040 period in McPherson et al. (2017), with overall correct prediction rates ranging from 85% to 92% according to the tick establishment thresholds (i.e., 1%, 5%, 10%, and 20%). However, we recognize that infection prevalence of blacklegged ticks with *B. burgdorferi* sensu stricto should be lower in the southern United States compared to the northern United States (Ginsberg et al., 2021). It has been shown that latitudinal variations in host-tick associations contributed to this north-south pattern, with high levels of tick infestation on highly efficient reservoir hosts for *B. burgdorferi* sensu stricto (i.e., rodents) in the north and high levels of tick infestation on inefficient reservoir hosts for *B. burgdorferi* sensu stricto (i.e., lizards) in the south (Ginsberg et al., 2021). Our model may have overestimated tick density in some areas across the southeastern United States considering the simulated habitat suitability patterns of hosts. While habitat quality for hosts was derived from a habitat suitability index based on the proportion of forests in this study, future integration of climate- and habitat-driven models of host distribution (such as species distribution models; Guisan and Thuiller, 2005) followed by a model validation procedure should improve the model predictions. The baseline distribution of uninfected lone star ticks was consistent with the predicted range of climatic suitability for the 2011–2040 period obtained in Sagurova et al. (2019), including southern Ontario (Canada). To date, reproducing populations of lone star ticks have not been found in Canada (Nelder et al., 2019). When compared to the Köppen-Geiger climate classification for the present-day (1980–2016) (Beck et al., 2018), the current climatically suitable areas for the blacklegged tick and the lone star tick fall into the following climate classes: (i) temperate climate without dry season and with hot summer (Cfa), (ii) cold climate without dry season and with hot summer (Dfa), and (iii) cold climate without dry season and with warm summer (Dfb). Finally, it should be noted that the model was initialized with theoretical starting locations of tick populations to begin simulations of northward range invasion under theoretical scenarios of increasing temperature. The choice of starting locations did not affect the final results of the spatial distribution patterns of infected blacklegged ticks and uninfected lone star ticks at the end of the simulations. However, a future version of the model should rely on both biologically realistic starting locations and plausible baseline scenarios of climate, socioeconomic and land use/land cover changes to simulate the true historical and recent progress of tick expansion in space and time.

4.2. Effects of increasing temperature on range spread of ticks and tick-borne pathogens

The predicted distribution patterns of blacklegged ticks and lone star ticks under the increasing temperature scenarios are in agreement with other studies and observations on the effects of a warmer climate on the northward range expansion of these two tick species (McPherson et al., 2017; Sagurova et al., 2019). In particular, warmer temperatures were predicted to expand the climatically suitable areas of Canada towards higher latitudes for the blacklegged tick and lone star tick, but the spatial extent and speed of the range expansion were found to be different between the two tick species. Compared with the baseline scenario, the future geographic extent of temperature suitability for

infected blacklegged ticks encompassed some parts of northern Quebec (including Nord-du-Québec, Saguenay-Lac-Saint-Jean, and Côte-Nord) and exceeded that for uninfected lone star ticks, with an increase in the extent of tick-infested areas reaching 31% for the blacklegged tick and 1% for the lone star tick under the increasing temperature scenarios. In the worst-case scenario of increasing temperature (i.e., increase of 600 degree-days), the speed of the northward invasion of infected blacklegged ticks increased to 61 km/year (range: 31 – 96 km/year), whereas uninfected lone star ticks spread at a lower rate of 23 km/year (range: 18 – 26 km/year). The results of the CA suggest that the differences observed in the extent to which the two tick species have shifted their geographic range northward were due to variations in the degree of attractiveness of resource-rich areas to migratory birds in the landscape, with a daily distance traveled by migratory birds carrying lone star ticks decreasing more rapidly with increasing resource availability in comparison with birds carrying blacklegged ticks. It is possible that parasitism by lone star ticks has greater negative impacts on health state of birds than parasitism by blacklegged ticks due to larger blood meals in lone star ticks (Koch and Sauer, 1984) and higher densities of feeding lone star ticks caused by their aggressive feeding behavior (Durden et al., 2001). Empirical studies have shown that stopover behavior of migratory birds and their departure decisions from stopover sites depended on their body condition combined with extrinsic factors (Covino et al., 2015; Jenni and Schaub, 2003). Birds in poor physical condition may stop more frequently and stay longer at stopover sites than birds in good physical condition (Duijns et al., 2017; Fusani et al., 2009). However, to date, blacklegged ticks and lone star ticks have not been used as model ectoparasites to test the effects of infestation levels on health state of birds, so that this hypothesis remains to be tested. Agent-based modeling offers an interesting opportunity to evaluate the relationship between tick infestation rates among individual birds and the speed of bird movement (see Tardy et al., 2022 for an example of agent-based models).

Our results suggest a higher contribution of long-distance migratory bird dispersal in the northward invasion process of blacklegged ticks compared to lone star ticks, which would be more reliant on local dispersal of terrestrial hosts. The baseline spatial patterns of infected blacklegged tick and uninfected lone star tick densities were associated with the habitat suitability patterns of hosts. Occurrence of these tick species depends on the presence of deer (Kilpatrick et al., 2014; Paddock and Yabsley, 2007). In particular, the white-tailed deer is considered as a keystone wildlife host for all parasitic stages of lone star ticks by acting both as a preferred food source and a mode of transport (Paddock and Yabsley, 2007), therefore contributing to the northward invasion of this tick species. With ongoing climate change, deer distribution is likely to expand northward due to milder winter conditions (i.e., less extreme temperatures and less snow) in conjunction with landscape changes that create early vegetation resource subsidies (Dawe and Boutin, 2016; Fisher et al., 2020). The existence of a strong link between lone star tick density and white-tailed deer availability has also been highlighted by several field studies that have evaluated the impacts of deer management (exclusion and topical treatment of deer with acaricides) (e.g., Bloemer et al., 1990; Pound et al., 2000). For example, the topical application of an acaricide to deer through the use of the "4-poster" device was found to be more effective in reducing lone star tick populations (nymph mortality of 99% and 95% observed at two study sites) compared to blacklegged ticks (nymph mortality of 69%, 76% and 80% observed at three study sites), which would be consistent with immature blacklegged ticks being less dependent on deer than immature lone star ticks (Carroll et al., 2003).

Differences in climatic requirements between these two tick species can also explain their contrasting spatial distribution and abundance patterns. Overall, lone star ticks display a lower resistance to cold conditions compared to blacklegged ticks (Nuttall, 2021), and it has been shown that the blacklegged tick was more vulnerable to desiccation than the lone star tick (Schulze et al., 2002). The future changes (2071 – 2100) in the Köppen-Geiger climate types (Beck et al., 2018) reveal that the future distributional areas for the two tick species will be governed by a cold climate without a dry season and with a warm summer (Dfb), becoming climatically suitable for ticks. Besides climate change, land use and land cover changes (not modeled in this study) in response to climate and socioeconomic changes can also affect abundance and distribution of tick populations. Whereas blacklegged ticks are adapted to temperate deciduous forests where humidity is high, the habitat associations are less clear for lone star ticks that can be present in forests, as well as in open-canopy and xeric habitats where the probability of encountering blacklegged ticks is low (reviewed in Mathisson et al., 2021). In the context of climate change, it is unknown if the Canadian boreal forest (i.e., the northernmost forest biome) is currently suitable for the two tick species. However, this forest is expected to be impacted by increasing temperatures associated with climate warming. In particular, wildfire activity that decreases the water retention capacity of soils by reducing the soil organic matter layer can modify forest composition by transforming forests dominated by mature evergreen conifers to forests dominated by young broadleaf deciduous stands (Mack et al., 2021; Wang et al., 2020), which could create improved conditions for ticks and their reproduction hosts in the future. In the context of socioeconomic changes, the creation of fragmented agroforestry landscapes can contribute to both increased tick densities and tick infection prevalence by promoting high densities of tick reproduction hosts (i.e., deer) and pathogen amplification hosts (i.e., rodents) (Allan et al., 2003; Brownstein et al., 2005). For example, in these landscapes, deer can benefit from both easier movement through a higher landscape connectivity and the presence of ecotonal habitats that offer better foraging opportunities (Clark and Gilbert, 1982; Walter et al., 2009). Deer populations are also abundant in semi-forested suburban areas given that these areas are free of hunting pressure and predators, and provide winter forage (Etter et al., 2002; Kilpatrick and Spohr, 2000). Other host animal species are also adaptable to these landscapes and can influence tick-borne disease risk. For example, increased predation by the coyote, *Canis latrans*, on a rodent mesopredator, the red fox (*Vulpes vulpes*), has been associated with increased abundance of rodents, and thus higher Lyme disease risk (Levi et al., 2012). The conversion of agroforestry landscapes to semi-forested suburban landscapes is thus likely to increase human exposure to infected ticks (Diuk-Wasser et al., 2020). In addition, findings resulting from an agent-based mechanistic model that considered future scenarios of combined changes in climate, socioeconomics and land use/land cover revealed that conversion of forest to agriculture is projected to decrease density of *B. burgdorferi* sensu lato-infected *Ixodes ricinus* nymphs in Mediterranean areas of southern Europe due to decreases in host densities (Li et al., 2019). The increasing temperature scenarios applied in this study confirm the possible importance of climate warming in increasing the geographic extent of climatically suitable areas for ticks and their pathogens, but it should be considered in conjunction with migratory bird movement behavior and mate-finding Allee effects, when seeking to predict the speed of infected tick invasion. In this study, only the relationship between the daily per capita mortality rate of ticks and annual CDD $> 0\ ^{\circ}C$ was investigated, while interactions of some model components involving host movement, host population dynamics and pathogen transmission may be affected by climate change (Ogden et al., 2021). However, empirical information on the sensitivity of host populations and pathogens to temperature changes are often not available, as is discussed in Li et al. (2016). Given these data challenges, we parameterized our model based on a CA due to uncertainties associated with some model input parameters.

Mechanistic models based on ordinary differential equations and partial differential equations have increasingly been applied to investigate the effects of climate warming on spatial spread of tick-borne diseases (reviewed in Lou and Wu, 2017; Norman et al., 2016; Ostfeld and Brunner, 2015). For example, the model of Ogden et al. (2005) provided a general theoretical framework for exploring the impacts of climate

change on tick population dynamics and tick-borne pathogen transmission cycles (Ludwig et al., 2016; Ogden et al., 2008a, 2007, 2006; Wallace et al., 2019), and for building prediction maps of the basic reproduction number (R_0) of ticks, a measure of tick population persistence, under current and future climate conditions in North America (McPherson et al., 2017; Ogden et al., 2014b; Wu et al., 2013). In particular, this model uses laboratory-derived relationships between tick life stage-specific development duration and temperature (Ogden et al., 2004) to estimate limits in mean annual degree-days above 0 °C for blacklegged tick establishment in Canada. However, most of these mechanistic models do not account for host movement across the landscape, while the benefits of adequately integrating movement ecology into spatial disease models have been highlighted in the literature (Boulinier et al., 2016; Fofana and Hurford, 2017). In particular, failure to integrate a mechanistic process of movement can be detrimental to contact estimation, and thus can lead to biased conclusions about pathogen persistence (Scherer et al., 2020). Even though we incorporated a less complex process of tick population dynamics (i.e., combining all tick life stages) into our model compared to existing models, we propose a general theoretical framework with a mechanistic representation of host movement, which can be used to generate current and future predictions of tick-borne disease spread risk at the continental scale under combined changes of climate, socioeconomics, and land use/land cover. In particular, a formulation of pathogen R_0, an epidemiological metric of the potential of pathogens to spread, can be extended to reaction-advection-diffusion models (Jiang et al., 2018; Wang et al., 2022). Future integration of more complex scenarios of climate, socioeconomic and land use/land cover changes may provide better understanding and thus predictions of tick-borne disease risk patterns under global environmental change. The application of our model to such scenarios will be an important next step in advancing this area of research.

Funding

This work was supported by the Public Health Agency of Canada.

CRediT authorship contribution statement

Olivia Tardy: Conceptualization, Methodology, Validation, Formal analysis, Investigation, Data curation, Writing – original draft, Writing – review & editing, Visualization, Supervision. **Emily Sohanna Acheson:** Investigation, Writing – review & editing. **Catherine Bouchard:** Conceptualization, Writing – review & editing, Supervision. **Éric Chamberland:** Methodology, Software, Resources. **André Fortin:** Methodology, Resources. **Nicholas H. Ogden:** Conceptualization, Writing – review & editing, Supervision, Funding acquisition. **Patrick A. Leighton:** Conceptualization, Writing – review & editing, Supervision.

Declaration of Competing Interest

None.

Data availability

Data will be made available on request.

Acknowledgments

We thank Calcul Québec (https://www.calculquebec.ca/) and Compute Canada (https://www.computecanada.ca/) for the computational resources. All simulations were run on the Cedar supercomputer located at the Simon Fraser University in British Columbia, Canada.

Supplementary materials

Supplementary materials associated with this article can be found, in the online version, at doi:10.1016/j.ttbdis.2023.102161.

References

Alerstam, T., 1993. Bird Migration. Cambridge University Press, Cambridge, England.
Allan, B.F., Keesing, F., Ostfeld, R.S., 2003. Effect of forest fragmentation on Lyme disease risk. Conserv. Biol. 17, 267–272. https://doi.org/10.1046/j.1523-1739.2003.01260.x.
Beck, H.E., Zimmermann, N.E., McVicar, T.R., Vergopolan, N., Berg, A., Wood, E.F., 2018. Present and future Köppen-Geiger climate classification maps at 1-km resolution. Sci. Data 5, 180214. https://doi.org/10.1038/sdata.2018.214.
Begon, M., Harper, J.L., Townsend, C.R., 1996. Ecology: Individuals, Populations and Communities, 3rd ed. Wiley-Blackwell, Oxford, UK.
Berthold, P., 2001. Bird Migration: A General Survey. Oxford University Press, New York, United States of America.
Bivand, R., Keitt, T., Rowlingson, B., 2022. Rgdal: bindings for the geospatial data abstraction library. R package version 1.5-31. https://CRAN.R-project.org/package=rgdal.
Bivand, R., Lewin-Koh, N., 2022. Maptools: tools for handling spatial objects. R package version 1.1-4. https://CRAN.R-project.org/package=maptools.
Bivand, R., Rundel, C., 2021. Rgeos: interface to geometry engine-open source (GEOS). R package version 0.5-9. https://CRAN.R-project.org/package=rgeos.
Bloemer, S.R., Mount, G.A., Morris, T.A., Zimmerman, R.H., Barnard, D.R., Snoddy, E.L., 1990. Management of lone star ticks (Acari: ixodidae) in recreational areas with acaricide applications, vegetative management, and exclusion of white-tailed deer. J. Med. Entomol. 27, 543–550. https://doi.org/10.1093/jmedent/27.4.543.
Bloemer, S.R., Zimmerman, R.H., Fairbanks, K., 1988. Abundance, attachment sites, and density estimators of lone star ticks (Acari: ixodidae) infesting white-tailed deer. J. Med. Entomol. 25, 295–300. https://doi.org/10.1093/jmedent/25.4.295.
Boulinier, T., Kada, S., Ponchon, A., Dupraz, M., Dietrich, M., Gamble, A., Bourret, V., Duriez, O., Bazire, R., Tornos, J., 2016. Migration, prospecting, dispersal? What host movement matters for infectious agent circulation? Integr. Comp. Biol. 56, 330–342. https://doi.org/10.1093/icb/icw015.
Brownstein, J.S., Skelly, D.K., Holford, T.R., Fish, D., 2005. Forest fragmentation predicts local scale heterogeneity of Lyme disease risk. Oecologia 146, 469–475. https://doi.org/10.1007/s00442-005-0251-9.
Carroll, J.F., Allen, P.C., Hill, D.E., Pound, J.M., Miller, J.A., George, J.E., 2003. Control of *Ixodes scapularis* and *Amblyomma americanum* through use of the '4-poster' treatment device on deer in Maryland. In: Jongejan, F., Kaufman, W.R. (Eds.), Ticks and Tick-Borne Pathogens. Springer, Dordrecht, Netherlands, pp. 289–296. https://doi.org/10.1007/978-94-017-3526-1_30.
Clark, T.P., Gilbert, F.F., 1982. Ecotones as a measure of deer habitat quality in central Ontario. J. Appl. Ecol. 19, 751–758. https://doi.org/10.2307/2403279.
Clow, K.M., Ogden, N.H., Lindsay, L.R., Michel, P., Pearl, D.L., Jardine, C.M., 2017. The influence of abiotic and biotic factors on the invasion of *Ixodes scapularis* in Ontario, Canada. Ticks Tick Borne Dis. 8, 554–563. 10.1016/j.ttbdis.2017.03.003.
Collins, C.R., Kays, R.W., 2014. Patterns of mortality in a wild population of white-footed mice. Northeast. Nat. 21, 323–336. https://doi.org/10.1656/045.021.0213.
Commins, S.P., James, H.R., Kelly, L.A., Pochan, S.L., Workman, L.J., Perzanowski, M.S., Kocan, K.M., Fahy, J.V., Nganga, L.W., Ronmark, E., Cooper, P.J., Platts-Mills, T.A. E., 2011. The relevance of tick bites to the production of IgE antibodies to the mammalian oligosaccharide galactose-α-1,3-galactose. J. Allergy Clin. Immunol. 127 https://doi.org/10.1016/j.jaci.2011.02.019, 1286-1293.e1286.
Covino, K.M., Holberton, R.L., Morris, S.R., 2015. Factors influencing migratory decisions made by songbirds on spring stopover. J. Avian Biol. 46, 73–80. https://doi.org/10.1111/jav.00463.
Daniels, T.J., Falco, R.C., Fish, D., 2000. Estimating population size and drag sampling efficiency for the blacklegged tick (Acari: ixodidae). J. Med. Entomol. 37, 357–363, 10.1603/0022-2585(2000)037[0357:EPSADS]2.0.CO;2.
Davis, S., Bent, S.J., 2011. Loop analysis for pathogens: niche partitioning in the transmission graph for pathogens of the North American tick *Ixodes scapularis*. J. Theor. Biol. 269, 96–103. https://doi.org/10.1016/j.jtbi.2010.10.011.
Dawe, K.L., Boutin, S., 2016. Climate change is the primary driver of white-tailed deer (*Odocoileus virginianus*) range expansion at the northern extent of its range; land use is secondary. Ecol. Evol. 6, 6435–6451. https://doi.org/10.1002/ece3.2316.
De La Fuente, J., Estrada-Pena, A., Venzal, J.M., Kocan, K.M., Sonenshine, D.E., 2008. Overview: ticks as vectors of pathogens that cause disease in humans and animals. Front. Biosci. 13, 6938–6946. https://doi.org/10.2741/3200.
Diuk-Wasser, M.A., VanAcker, M.C., Fernandez, M.P., 2020. Impact of land use changes and habitat fragmentation on the eco-epidemiology of tick-borne diseases. J. Med. Entomol. 58, 1546–1564. https://doi.org/10.1093/jme/tjaa209.
Duijns, S., Niles, L.J., Dey, A., Aubry, Y., Friis, C., Koch, S., Anderson, A.M., Smith, P.A., 2017. Body condition explains migratory performance of a long-distance migrant. Proc. R. Soc. B 284, 20171374. https://doi.org/10.1098/rspb.2017.1374.
Dumas, A., Bouchard, C., Dibernardo, A., Drapeau, P., Lindsay, L.R., Ogden, N.H., Leighton, P.A., 2022. Transmission patterns of tick-borne pathogens among birds and rodents in a forested park in southeastern Canada. PLoS ONE 17, e0266527. https://doi.org/10.1371/journal.pone.0266527.
Durden, L.A., Oliver, J.H., Kinsey, A.A., 2001. Ticks (Acari: ixodidae) and spirochetes (Spirochaetaceae: spirochaetales) recovered from birds on a Georgia barrier Island. J. Med. Entomol. 38, 231–236. https://doi.org/10.1603/0022-2585-38.2.231.

Eisen, R.J., Eisen, L., 2018. The blacklegged tick, *Ixodes scapularis*: an increasing public health concern. Trends Parasitol 34, 295–309. https://doi.org/10.1016/j.pt.2017.12.006.

Eisen, R.J., Eisen, L., Beard, C.B., 2016. County-scale distribution of *Ixodes scapularis* and *Ixodes pacificus* (Acari: ixodidae) in the continental United States. J. Med. Entomol. 53, 349–386. https://doi.org/10.1093/jme/tjv237.

Eisen, R.J., Kugeler, K.J., Eisen, L., Beard, C.B., Paddock, C.D., 2017. Tick-borne zoonoses in the United States: persistent and emerging threats to human health. ILAR J 58, 319–335. https://doi.org/10.1093/ilar/ilx005.

Elith, J., Leathwick, J.R., Hastie, T., 2008. A working guide to boosted regression trees. J. Anim. Ecol. 77, 802–813. https://doi.org/10.1111/j.1365-2656.2008.01390.x.

Etter, D.R., Hollis, K.M., Van Deelen, T.R., Ludwig, D.R., Chelsvig, J.E., Anchor, C.L., Warner, R.E., 2002. Survival and movements of white-tailed deer in suburban Chicago. Illinois. J. Wildl. Manage. 66, 500–510. https://doi.org/10.2307/3803183.

Fisher, J.T., Burton, A.C., Nolan, L., Roy, L., 2020. Influences of landscape change and winter severity on invasive ungulate persistence in the Nearctic boreal forest. Sci. Rep. 10, 8742. https://doi.org/10.1038/s41598-020-65385-3.

Fofana, A.M., Hurford, A., 2017. Mechanistic movement models to understand epidemic spread. Philos. Trans. R. Soc. Lond. B Biol. Sci. 372, 20160086 https://doi.org/10.1098/rstb.2016.0086.

Fowler, P.D., Nguyentran, S., Quatroche, L., Porter, M.L., Kobbekaduwa, V., Tippin, S., Miller, G., Dinh, E., Foster, E., Tsao, J.I., 2022. Northward expansion of *Amblyomma americanum* (Acari: ixodidae) into southwestern Michigan. J. Med. Entomol. 59, 1646–1659. https://doi.org/10.1093/jme/tjac082.

Fusani, L., Cardinale, M., Carere, C., Goymann, W., 2009. Stopover decision during migration: physiological conditions predict nocturnal restlessness in wild passerines. Biol. Lett. 5, 302–305. https://doi.org/10.1098/rsbl.2008.0755.

Gilbert, L., 2021. The impacts of climate change on ticks and tick-borne disease risk. Annu. Rev. Entomol. 66, 373–388. https://doi.org/10.1146/annurev-ento-052720-094533.

Ginsberg, H.S., Hickling, G.J., Burke, R.L., Ogden, N.H., Beati, L., LeBrun, R.A., Arsnoe, I. M., Gerhold, R., Han, S., Jackson, K., Maestas, L., Moody, T., Pang, G., Ross, B., Rulison, E.L., Tsao, J.I., 2021. Why Lyme disease is common in the northern US, but rare in the south: the roles of host choice, host-seeking behavior, and tick density. PLoS Biol 19, e3001066. https://doi.org/10.1371/journal.pbio.3001066.

Ginsberg, H.S., Rulison, E.L., Miller, J.L., Pang, G., Arsnoe, I.M., Hickling, G.J., Ogden, N. H., LeBrun, R.A., Tsao, J.I., 2020. Local abundance of *Ixodes scapularis* in forests: effects of environmental moisture, vegetation characteristics, and host abundance. Ticks Tick Borne Dis. 11, 101271 https://doi.org/10.1016/j.ttbdis.2019.101271.

Ginsberg, H.S., Zhioua, E., 1996. Nymphal survival and habitat distribution of *Ixodes scapularis* and *Amblyomma americanum* ticks (Acari: ixodidae) on Fire Island, New York, USA. Exp. Appl. Acarol. 20, 533–544. https://doi.org/10.1007/BF00048285.

Goddard, J., Varela-Stokes, A.S., 2009. Role of the lone star tick, *Amblyomma americanum* (L.), in human and animal diseases. Vet. Parasitol. 160, 1–12. https://doi.org/10.1016/j.vetpar.2008.10.089.

Green, M.L., Kelly, A.C., Satterthwaite-Phillips, D., Manjerovic, M.B., Shelton, P., Novakofski, J., Mateus-Pinilla, N., 2017. Reproductive characteristics of female white-tailed deer (*Odocoileus virginianus*) in the Midwestern USA. Theriogenology 94, 71–78. https://doi.org/10.1016/j.theriogenology.2017.02.010.

Guerra, M., Walker, E., Jones, C., Paskewitz, S., Cortinas, M.R., Stancil, A., Beck, L., Bobo, M., Kitron, U., 2002. Predicting the risk of Lyme disease: habitat suitability for *Ixodes scapularis* in the north central United States. Emerg. Infect. Dis. 8, 289–297. https://doi.org/10.3201/eid0803.010166.

Guillot, C., Badcock, J., Clow, K., Cram, J., Dergousoff, S., Dibernardo, A., Evason, M., Fraser, E., Galanis, E., Gasmi, S., German, G.J., Howse, D.T., Jardine, C., Jenkins, E., Koffi, J., Kulkarni, M., Lindsay, L.R., Lumsden, G., McKay, R., Moore, K., Morshed, M., Munn, D., Nelder, M., Nocera, J., Ripoche, M., Rochon, K., Russell, C., Slatculescu, A., Talbot, B., Thivierge, K., Voordouw, M., Bouchard, C., Leighton, P., 2020. Sentinel surveillance of Lyme disease risk in Canada, 2019: results from the first year of the Canadian Lyme Sentinel Network (CaLSeN). Can. Commun. Dis. Rep. 46, 354–361. https://doi.org/10.14745/ccdr.v46i10a08.

Guisan, A., Thuiller, W., 2005. Predicting species distribution: offering more than simple habitat models. Ecol. Lett. 8, 993–1009. https://doi.org/10.1111/j.1461-0248.2005.00792.x.

Hartfield, M., White, K.A.J., Kurtenbach, K., 2011. The role of deer in facilitating the spatial spread of the pathogen *Borrelia burgdorferi*. Theor. Ecol. 4, 27–36. https://doi.org/10.1007/s12080-010-0072-2.

Hengge, U.R., Tannapfel, A., Tyring, S.K., Erbel, R., Arendt, G., Ruzicka, T., 2003. Lyme borreliosis. Lancet Infect. Dis. 3, 489–500. https://doi.org/10.1016/S1473-3099(03)00722-9.

Hijmans, R.J., 2022. Raster: geographic data analysis and modeling. R package version 3.5-15. https://CRAN.R-project.org/package=raster.

Hijmans, R.J., Phillips, S., Leathwick, J., Elith, J., 2020. Dismo: species distribution modeling. R package version 1.3-3. https://CRAN.R-project.org/package=dismo.

Hilker, F.M., Langlais, M., Petrovskii, S.V., Malchow, H., 2007. A diffusive SI model with Allee effect and application to FIV. Math. Biosci. 206, 61–80. https://doi.org/10.1016/j.mbs.2005.10.003.

Jenni, L., Schaub, M., 2003. Behavioural and physiological reactions to environmental variation in bird migration: a review. In: Berthold, P., Gwinner, E., Sonnenschein, E. (Eds.), Avian Migration. Springer Berlin Heidelberg, Berlin, Germany, pp. 155–171. https://doi.org/10.1007/978-3-662-05957-9_10.

Jiang, D., Wang, Z.-C., Zhang, L., 2018. A reaction-diffusion-advection SIS epidemic model in a spatially-temporally heterogeneous environment. Discrete Contin. Dyn. Syst. B 23, 4557–4578. https://doi.org/10.3934/dcdsb.2018176.

Jongejan, F., Uilenberg, G., 2004. The global importance of ticks. Parasitology 129, S3–S14. https://doi.org/10.1017/S0031182004005967.

Jouffray, J.-.B., Wedding, L.M., Norström, A.V., Donovan, M.K., Williams, G.J., Crowder, L.B., Erickson, A.L., Friedlander, A.M., Graham, N.A.J., Gove, J.M., Kappel, C.V., Kittinger, J.N., Lecky, J., Oleson, K.L.L., Selkoe, K.A., White, C., Williams, I.D., Nyström, M., 2019. Parsing human and biophysical drivers of coral reef regimes. Proc. R. Soc. B 286, 20182544. https://doi.org/10.1098/rspb.2018.2544.

Keesing, F., Brunner, J., Duerr, S., Killilea, M., LoGiudice, K., Schmidt, K., Vuong, H., Ostfeld, R.S., 2009. Hosts as ecological traps for the vector of Lyme disease. Proc. R. Soc. B 276, 3911–3919. https://doi.org/10.1098/rspb.2009.1159.

Kilpatrick, H.J., Labonte, A.M., Stafford III, K.C., 2014. The relationship between deer density, tick abundance, and human cases of Lyme disease in a residential community. J. Med. Entomol. 51, 777–784. https://doi.org/10.1603/ME13232.

Kilpatrick, H.J., Spohr, S.M., 2000. Spatial and temporal use of a suburban landscape by female white-tailed deer. Wildl. Soc. Bull. 28, 1023–1029.

Koch, H.G., 1984. Survival of the lone star tick, *Amblyomma americanum* (Acari: ixodidae), in contrasting habitats and different years in southeastern Oklahoma, USA. J. Med. Entomol. 21, 69–79. https://doi.org/10.1093/jmedent/21.1.69.

Koch, H.G., Sauer, J.R., 1984. Quantity of blood ingested by four species of hard ticks (Acari: ixodidae) fed on domestic dogs. Ann. Entomol. Soc. Am. 77, 142–146. https://doi.org/10.1093/aesa/77.2.142.

Lado, P., Smith, M.L., Carstens, B.C., Klompen, H., 2020. Population genetic structure and demographic history of the lone star tick, *Amblyomma americanum* (Ixodida: ixodidae): new evidence supporting old records. Mol. Ecol. 29, 2810–2823. https://doi.org/10.1111/mec.15524.

Leighton, P.A., Koffi, J.K., Pelcat, Y., Lindsay, L.R., Ogden, N.H., 2012. Predicting the speed of tick invasion: an empirical model of range expansion for the Lyme disease vector *Ixodes scapularis* in Canada. J. Appl. Ecol. 49, 457–464. https://doi.org/10.1111/j.1365-2664.2012.02112.x.

Levi, T., Kilpatrick, A.M., Mangel, M., Wilmers, C.C., 2012. Deer, predators, and the emergence of Lyme disease. Proc. Natl. Acad. Sci. U. S. A. 109, 10942–10947. https://doi.org/10.1073/pnas.1204536109.

Li, S., Gilbert, L., Harrison, P.A., Rounsevell, M.D.A., 2016. Modelling the seasonality of Lyme disease risk and the potential impacts of a warming climate within the heterogeneous landscapes of Scotland. J. Royal Soc. Interface 13, 20160140. https://doi.org/10.1098/rsif.2016.0140.

Li, S., Gilbert, L., Vanwambeke, S.O., Yu, J., Purse, B.V., Harrison, P.A., 2019. Lyme disease risks in Europe under multiple uncertain drivers of change. Environ. Health Perspect. 127, 067010 https://doi.org/10.1289/EHP4615.

Lindsay, L.R., Mathison, S.W., Barker, I.K., McEwen, S.A., Gillespie, T.J., Surgeoner, G.A., 1999. Microclimate and habitat in relation to *Ixodes scapularis* (Acari: ixodidae) populations on long point, Ontario, Canada. J. Med. Entomol. 36, 255–262. https://doi.org/10.1093/jmedent/36.3.255.

LoGiudice, K., Ostfeld, R.S., Schmidt, K.A., Keesing, F., 2003. The ecology of infectious disease: effects of host diversity and community composition on Lyme disease risk. Proc. Natl. Acad. Sci. U. S. A. 100, 567–571. https://doi.org/10.1073/pnas.0233733100.

Lou, Y., Wu, J., 2017. Modeling lyme disease transmission. Infect. Dis. Model. 2, 229–243. https://doi.org/10.1016/j.idm.2017.05.002.

Ludwig, A., Ginsberg, H.S., Hickling, G.J., Ogden, N.H., 2016. A Dynamic population model to investigate effects of climate and climate-independent factors on the lifecycle of *Amblyomma americanum* (Acari: ixodidae). J. Med. Entomol. 53, 99–115. https://doi.org/10.1093/jme/tjv150.

Mack, M.C., Walker, X.J., Johnstone, J.F., Alexander, H.D., Melvin, A.M., Jean, M., Miller, S.N., 2021. Carbon loss from boreal forest wildfires offset by increased dominance of deciduous trees. Science 372, 280–283. https://doi.org/10.1126/science.abf3903.

Madhav, N.K., Brownstein, J.S., Tsao, J.I., Fish, D., 2004. A dispersal model for the range expansion of blacklegged tick (Acari: ixodidae). J. Med. Entomol. 41, 842–852. https://doi.org/10.1603/0022-2585-41.5.842.

Madison-Antenucci, S., Kramer, L.D., Gebhardt, L.L., Kauffman, E., 2020. Emerging tick-borne diseases. Clin. Microbiol. Rev. 33 https://doi.org/10.1128/CMR.00083-18.

Mangan, M.J., Foré, S.A., Kim, H.-.J., 2018. Ecological modeling over seven years to describe the number of host-seeking *Amblyomma americanum* in each life stage in northeast Missouri. J. Vector Ecol. 43, 271–284. https://doi.org/10.1111/jvec.12311.

Mathisson, D.C., Kross, S.M., Palmer, M.I., Diuk-Wasser, M.A., 2021. Effect of vegetation on the abundance of tick vectors in the northeastern United States: a review of the literature. J. Med. Entomol. 58, 2030–2037. https://doi.org/10.1093/jme/tjab098.

McPherson, M., García-García, A., Cuesta-Valero, F.J., Beltrami, H., Hansen-Ketchum, P., MacDougall, D., Ogden, N.H., 2017. Expansion of the Lyme disease vector *Ixodes scapularis* in Canada inferred from CMIP5 climate projections. Environ. Health Perspect. 125, 057008 https://doi.org/10.1289/EHP57.

McShea, W.J., Schwede, G., 1993. Variable acorn crops: responses of white-tailed deer and other mast consumers. J. Mammal. 74, 999–1006. https://doi.org/10.2307/1382439.

Moorcroft, P.R., Lewis, M.A., 2006. Mechanistic Home Range Analysis. Princeton University Press, Princeton, NJ, USA.

Mount, G.A., Haile, D.G., Daniels, E., 1997. Simulation of blacklegged tick (Acari: ixodidae) population dynamics and transmission of *Borrelia burgdorferi*. J. Med. Entomol. 34, 461–484. https://doi.org/10.1093/jmedent/34.4.461.

Needham, G.R., Teel, P.D., 1991. Off-host physiological ecology of ixodid ticks. Annu. Rev. Entomol. 36, 659–681. https://doi.org/10.1146/annurev.en.36.010191.003303.

Nelder, M.P., Russell, C.B., Clow, K.M., Johnson, S., Weese, J.S., Cronin, K., Ralevski, F., Jardine, C.M., Patel, S.N., 2019. Occurrence and distribution of *Ambylomma*

americanum as determined by passive surveillance in Ontario, Canada (1999–2016). Ticks Tick Borne Dis 10, 146–155. https://doi.org/10.1016/j.ttbdis.2018.10.001.
Nelson, M.E., Mech, L.D., 1986. Mortality of white-tailed deer in northeastern Minnesota. J. Wildl. Manage. 50, 691–698. https://doi.org/10.2307/3800983.
Norman, R.A., Worton, A.J., Gilbert, L., 2016. Past and future perspectives on mathematical models of tick-borne pathogens. Parasitology 143, 850–859. https://doi.org/10.1017/S0031182015001523.
Nuttall, P., 2021. Climate, ticks and disease. University of Oxford, Oxford, England.
Ogden, N.H., Barker, I.K., Francis, C.M., Heagy, A., Lindsay, L.R., Hobson, K.A., 2015. How far north are migrant birds transporting the tick *Ixodes scapularis* in Canada? Insights from stable hydrogen isotope analyses of feathers. Ticks Tick Borne Dis. 6, 715–720. https://doi.org/10.1016/j.ttbdis.2015.06.004.
Ogden, N.H., Ben Beard, C., Ginsberg, H.S., Tsao, J.I., 2021. Possible effects of climate change on ixodid ticks and the pathogens they transmit: predictions and observations. J. Med. Entomol. 58, 1536–1545. https://doi.org/10.1093/jme/tjaa220.
Ogden, N.H., Bigras-Poulin, M., Hanincová, K., Maarouf, A., O'Callaghan, C.J., Kurtenbach, K., 2008a. Projected effects of climate change on tick phenology and fitness of pathogens transmitted by the North American tick *Ixodes scapularis*. J. Theor. Biol. 254, 621–632. https://doi.org/10.1016/j.jtbi.2008.06.020.
Ogden, N.H., Bigras-Poulin, M., O'Callaghan, C.J., Barker, I.K., Lindsay, L.R., Maarouf, A., Smoyer-Tomic, K.E., Waltner-Toews, D., Charron, D., 2005. A dynamic population model to investigate effects of climate on geographic range and seasonality of the tick *Ixodes scapularis*. Int. J. Parasitol. 35, 375–389. https://doi.org/10.1016/j.ijpara.2004.12.013.
Ogden, N.H., Bigras-Poulin, M., O'Callaghan, C.J., Barker, I.K., Kurtenbach, K., Lindsay, L.R., Charron, D.F., 2007. Vector seasonality, host infection dynamics and fitness of pathogens transmitted by the tick *Ixodes scapularis*. Parasitology 134, 209–227. https://doi.org/10.1017/s0031182006001417.
Ogden, N.H., Bouchard, C., Kurtenbach, K., Margos, G., Lindsay, L.R., Trudel, L., Nguon, S., Milord, F., 2010. Active and passive surveillance and phylogenetic analysis of *Borrelia burgdorferi* elucidate the process of Lyme disease risk emergence in Canada. Environ. Health Perspect. 118, 909–914. https://doi.org/10.1289/ehp.0901766.
Ogden, N.H., Koffi, J.K., Pelcat, Y., Lindsay, L.R., 2014a. Environmental risk from Lyme disease in central and eastern Canada: a summary of recent surveillance information. Can. Commun. Dis. Rep. 40, 74–82. https://doi.org/10.14745/ccdr.v40i05a01.
Ogden, N.H., Lindsay, L.R., Beauchamp, G., Charron, D., Maarouf, A., O'Callaghan, C.J., Waltner-Toews, D., Barker, I.K., 2004. Investigation of relationships between temperature and developmental rates of tick *Ixodes scapularis* (Acari: ixodidae) in the laboratory and field. J. Med. Entomol. 41, 622–633. https://doi.org/10.1603/0022-2585-41.4.622.
Ogden, N.H., Lindsay, L.R., Hanincová, K., Barker, I.K., Bigras-Poulin, M., Charron, D.F., Heagy, A., Francis, C.M., O'Callaghan, C.J., Schwartz, I., 2008b. Role of migratory birds in introduction and range expansion of *Ixodes scapularis* ticks and of *Borrelia burgdorferi* and *Anaplasma phagocytophilum* in Canada. Appl. Environ. Microbiol. 74, 1780–1790. https://doi.org/10.1128/AEM.01982-07.
Ogden, N.H., Lindsay, L.R., Leighton, P.A., 2013a. Predicting the rate of invasion of the agent of Lyme disease *Borrelia burgdorferi*. J. Appl. Ecol. 50, 510–518. https://doi.org/10.1111/1365-2664.12050.
Ogden, N.H., Maarouf, A., Barker, I.K., Bigras-Poulin, M., Lindsay, L.R., Morshed, M.G., O'callaghan, C.J., Ramay, F., Waltner-Toews, D., Charron, D.F., 2006. Climate change and the potential for range expansion of the Lyme disease vector *Ixodes scapularis* in Canada. Int. J. Parasitol. 36, 63–70. https://doi.org/10.1016/j.ijpara.2005.08.016.
Ogden, N.H., Mechai, S., Margos, G., 2013b. Changing geographic ranges of ticks and tick-borne pathogens: drivers, mechanisms and consequences for pathogen diversity. Front. Cell. Infect. Microbiol. 3, 46. https://doi.org/10.3389/fcimb.2013.00046.
Ogden, N.H., Radojevic, M., Wu, X., Duvvuri, V.R., Leighton, P.A., Wu, J., 2014b. Estimated effects of projected climate change on the basic reproductive number of the Lyme disease vector *Ixodes scapularis*. Environ. Health Perspect. 122, 631–638. https://doi.org/10.1289/ehp.1307799.
Ostfeld, R.S., Brunner, J.L., 2015. Climate change and *Ixodes* tick-borne diseases of humans. Philos. Trans. R. Soc. Lond. B Biol. Sci. 370, 20140051 https://doi.org/10.1098/rstb.2014.0051.
Ostfeld, R.S., Schauber, E.M., Canham, C.D., Keesing, F., Jones, C.G., Wolff, J.O., 2001. Effects of acorn production and mouse abundance on abundance and *Borrelia burgdorferi* infection prevalence of nymphal *Ixodes scapularis* ticks. Vector Borne Zoonot. Dis 1, 55–63. https://doi.org/10.1089/153036601750137688.
Paddock, C.D., Yabsley, M.J., 2007. Ecological havoc, the rise of white-tailed deer, and the emergence of *Amblyomma americanum*-associated zoonoses in the United States. In: Childs, J.E., Mackenzie, J.S., Richt, J.A. (Eds.), Wildlife and Emerging Zoonotic Diseases: The Biology, Circumstances and Consequences of Cross-Species Transmission. Springer Berlin Heidelberg, Berlin, Germany, pp. 289–324. https://doi.org/10.1007/978-3-540-70962-6_12.
Pebesma, E., 2018. Simple features for R: standardized support for spatial vector data. R J 10, 439–446. https://doi.org/10.32614/RJ-2018-009.
Pebesma, E.J., 2004. Multivariable geostatistics in S: the gstat package. Comput. Geosci. 30, 683–691. https://doi.org/10.1016/j.cageo.2004.03.012.
Pinsky, M.L., Byler, D., 2015. Fishing, fast growth and climate variability increase the risk of collapse. Proc. R. Soc. B 282, 20151053. https://doi.org/10.1098/rspb.2015.1053.
Pound, J.M., Miller, J.A., George, J.E., Lemeilleur, C.A., 2000. The '4-poster'passive topical treatment device to apply acaricide for controlling ticks (Acari: ixodidae) feeding on white-tailed deer. J. Med. Entomol. 37, 588–594. https://doi.org/10.1603/0022-2585-37.4.588.
Development Core Team, R., 2019. R: a Language and Environment For Statistical Computing. R Foundation for Statistical Computing, Vienna, Austria. http://www.R-project.org.
Raghavan, R.K., Peterson, A.T., Cobos, M.E., Ganta, R., Foley, D., 2019. Current and future distribution of the lone star tick, *Amblyomma americanum* (L.) (Acari: ixodidae) in North America. PLoS ONE 14, e0209082. https://doi.org/10.1371/journal.pone.0209082.
Rand, P.W., Lubelczyk, C., Lavigne, G.R., Elias, S., Holman, M.S., Lacombe, E.H., Smith, R.P., 2003. Deer density and the abundance of *Ixodes scapularis* (Acari: ixodidae). J. Med. Entomol. 40, 179–184. https://doi.org/10.1603/0022-2585-40.2.179.
Rodewald, P., 2015. The Birds of North America. Cornell Laboratory of Ornithology, Ithaca, United States of America. https://birdsna.org.
Roy-Dufresne, E., Logan, T., Simon, J.A., Chmura, G.L., Millien, V., 2013. Poleward expansion of the white-footed mouse (*Peromyscus leucopus*) under climate change: implications for the spread of Lyme disease. PLoS ONE 8, e80724. https://doi.org/10.1371/journal.pone.0080724.
Sagurova, I., Ludwig, A., Ogden, N.H., Pelcat, Y., Dueymes, G., Gachon, P., 2019. Predicted northward expansion of the geographic range of the tick vector *Amblyomma americanum* in North America under future climate conditions. Environ. Health Perspect. 127, 107014 https://doi.org/10.1289/EHP5668.
Schaub, M., Jenni, L., 2001. Stopover durations of three warbler species along their autumn migration route. Oecologia 128, 217–227. https://doi.org/10.1007/s004420100654.
Scherer, C., Radchuk, V., Franz, M., Thulke, H.-.H., Lange, M., Grimm, V., Kramer-Schadt, S., 2020. Moving infections: individual movement decisions drive disease persistence in spatially structured landscapes. Oikos 129, 651–667. https://doi.org/10.1111/oik.07002.
Schulze, T.L., Jordan, R.A., Hung, R.W., 1995. Suppression of subadult *Ixodes scapularis* (Acari: ixodidae) following removal of leaf litter. J. Med. Entomol. 32, 730–733. https://doi.org/10.1093/jmedent/32.5.730.
Schulze, T.L., Jordan, R.A., Hung, R.W., 2002. Effects of microscale habitat physiognomy on the focal distribution of *Ixodes scapularis* and *Amblyomma americanum* (Acari: ixodidae) nymphs. Environ. Entomol. 31, 1085–1090. https://doi.org/10.1603/0046-225X-31.6.1085.
Simon, J.A., Marrotte, R.R., Desrosiers, N., Fiset, J., Gaitan, J., Gonzalez, A., Koffi, J.K., Lapointe, F.-.J., Leighton, P.A., Lindsay, L.R., Logan, T., Milord, F., Ogden, N.H., Rogic, A., Roy-Dufresne, E., Suter, D., Tessier, N., Millien, V., 2014. Climate change and habitat fragmentation drive the occurrence of *Borrelia burgdorferi*, the agent of Lyme disease, at the northeastern limit of its distribution. Evol. Appl. 7, 750–764. https://doi.org/10.1111/eva.12165.
Sonenshine, D.E., 2006. Tick pheromones and their use in tick control. Annu. Rev. Entomol. 51, 557–580. https://doi.org/10.1146/annurev.ento.51.110104.151150.
Sonenshine, D.E., 2018. Range expansion of tick disease vectors in North America: implications for spread of tick-borne disease. Int. J. Environ. Res. Public Health. 15, 478. https://doi.org/10.3390/ijerph15030478.
Springer, Y.P., Eisen, L., Beati, L., James, A.M., Eisen, R.J., 2014. Spatial distribution of counties in the continental United States with records of occurrence of *Amblyomma americanum* (Ixodida: ixodidae). J. Med. Entomol. 51, 342–351. https://doi.org/10.1603/ME13115.
Stafford III, K.C., Molaei, G., Little, E.A.H., Paddock, C.D., Karpathy, S.E., Labonte, A.M., 2018. Distribution and establishment of the lone star tick in Connecticut and implications for range expansion and public health. J. Med. Entomol. 55, 1561–1568. https://doi.org/10.1093/jme/tjy115.
Stafford III, K.C., Williams, S.C., 2017. Deer-targeted methods: a review of the use of topical acaricides for the control of ticks on white-tailed deer. J. Integr. Pest Manag. 8, 19. https://doi.org/10.1093/jipm/pmx014.
Tardy, O., Bouchard, C., Chamberland, E., Fortin, A., Lamirande, P., Ogden, N.H., Leighton, P.A., 2021. Mechanistic movement models reveal ecological drivers of tick-borne pathogen spread. J. Royal Soc. Interface 18, 20210134. https://doi.org/10.1098/rsif.2021.0134.
Tardy, O., Vincenot, C.E., Bouchard, C., Ogden, N.H., Leighton, P.A., 2022. Context-dependent host dispersal and habitat fragmentation determine heterogeneity in infected tick burdens: an agent-based modelling study. R. Soc. Open Sci. 9, 220245 https://doi.org/10.1098/rsos.220245.
Thiele, J.C., Kurth, W., Grimm, V., 2014. Facilitating parameter estimation and sensitivity analysis of agent-based models: a cookbook using NetLogo and R. J. Artif. Soc. Soc. Simul. 17, 11. https://doi.org/10.18564/jasss.2503.
Tsao, J.I., Hamer, S.A., Han, S., Sidge, J.L., Hickling, G.J., 2021. The contribution of wildlife hosts to the rise of ticks and tick-borne diseases in North America. J. Med. Entomol. 58, 1565–1587. https://doi.org/10.1093/jme/tjab047.
Wallace, D., Ratti, V., Kodali, A., Winter, J.M., Ayres, M.P., Chipman, J.W., Aoki, C.F., Osterberg, E.C., Silvanic, C., Partridge, T.F., Webb, M.J., 2019. Effect of rising temperature on Lyme disease: *ixodes scapularis* population dynamics and *Borrelia burgdorferi* transmission and prevalence. Can. J. Infect. Dis. Med. Microbiol. 2019, 9817930 https://doi.org/10.1155/2019/9817930.
Walter, W.D., VerCauteren, K.C., Campa, H., Clark, W.R., Fischer, J.W., Hygnstrom, S.E., Mathews, N.E., Nielsen, C.K., Schauber, E.M., Van Deelen, T.R., Winterstein, S.R., 2009. Regional assessment on influence of landscape configuration and connectivity

on range size of white-tailed deer. Landsc. Ecol. 24, 1405–1420. https://doi.org/10.1007/s10980-009-9374-4.

Wang, J.A., Sulla-Menashe, D., Woodcock, C.E., Sonnentag, O., Keeling, R.F., Friedl, M. A., 2020. Extensive land cover change across Arctic–Boreal Northwestern North America from disturbance and climate forcing. Glob. Change Biol. 26, 807–822. https://doi.org/10.1111/gcb.14804.

Wang, X., Wu, R., Zhao, X.-.Q., 2022. A reaction-advection-diffusion model of cholera epidemics with seasonality and human behavior change. J. Math. Biol. 84, 34. https://doi.org/10.1007/s00285-022-01733-3.

Watts, A.G., Saura, S., Jardine, C., Leighton, P., Werden, L., Fortin, M.-.J., 2018. Host functional connectivity and the spread potential of Lyme disease. Landsc. Ecol. 33, 1925–1938. https://doi.org/10.1007/s10980-018-0715-z.

Wolff, J.O., 1985. Comparative population ecology of *Peromyscus leucopus* and *Peromyscus maniculatus*. Can. J. Zool. 63, 1548–1555. https://doi.org/10.1139/z85-230.

Wu, X., Duvvuri, V.R., Lou, Y., Ogden, N.H., Pelcat, Y., Wu, J., 2013. Developing a temperature-driven map of the basic reproductive number of the emerging tick vector of Lyme disease *Ixodes scapularis* in Canada. J. Theor. Biol. 319, 50–61. https://doi.org/10.1016/j.jtbi.2012.11.014.

Zuur, A.F., Ieno, E.N., Smith, G.M., 2007. Analyzing Ecological Data. Springer, New York, United States of America. https://doi.org/10.1007/978-0-387-45972-1.